Neurobiology of Stress 36 (2025) 100726

Contents lists available at ScienceDirect

Neurobiology of Stress

journal homepage: www.elsevier.com/locate/ynstr

Early-life adversities compromise behavioral development in male and female mice heterozygous for CNTNAP2

Gabriele Chelini [a,*,1], Tommaso Fortunato-Asquini [a], Enrica Cerilli [a], Katia Monsorno [b], Benedetta Catena [a], Ginevra Matilde Dall'O' [a], Rosa Chiara Paolicelli [b], Yuri Bozzi [a,**]

[a] Center for Mind/Brain Sciences, University of Trento, Piazza della Manifattura n.1, 38068, Rovereto, TN, Italy
[b] Department of Biomedical Sciences, University of Lausanne, Rue du Bugnon n.7, CH-1005, Lausanne, Switzerland

ARTICLE INFO

Handling Editor: Prof R Lawrence Reagan

ABSTRACT

The etiological complexity of psychiatric disorders arises from the dynamic interplay between genetic and environmental vulnerabilities. Among the environmental components, early-life adversities are a major risk factor for developing a psychiatric condition. Yet, the interaction between adversities early in life and genetic vulnerability contributing to psychopathology is poorly understood. To fill this gap, we took advantage of the ideally controlled conditions of a pre-clinical approach. We raised a mouse model with genetic predisposition for multiple psychiatric disorders (autism spectrum, schizophrenia, bipolar disorder), the *Cntnap2*$^{+/-}$ mouse, with limited bedding and nesting (LBN), a well-established paradigm to induce early-life stress in rodents. These mice were compared to LBN-raised *Cntnap2*$^{+/+}$ littermates, as well as parallel groups of *Cntnap2*$^{+/+}$ and *Cntnap2*$^{+/-}$ raised in standard conditions. Using a battery for behavioral phenotyping we show that early-life adverse experience shapes non-overlapping phenotypic landscapes based on genetic predisposition. Specifically, LBN-raised *Cntnap2*$^{+/-}$ mice displayed a perseverative risk-taking behavior in the elevated plus maze. Interestingly, this trait was highly predictive of their success in social interaction, suggesting that the intrusion of anxiety into the social behavioral domain may contribute to extreme gain- or loss-of function in sociability. Finally, we show that LBN promotes hypertrophy of post-synaptic densities in the basolateral nucleus of the amygdala (BLA), but only in *Cntnap2*$^{+/-}$ raised in LBN this is associated with microglia abnormalities. We conclude that the interplay between early-life adversities and *Cntnap2* haploinsufficiency alters emotion regulation in mice, putatively as a consequence of deficient synaptic scaling in the BLA.

1. Introduction

Adverse childhood experience and genetic vulnerabilities are major risk factors for the development of psychiatric disorders (Caspi and Moffitt, 2006; Musci et al., 2019), but their mechanistic interaction contributing to psychopathology is largely understudied. This is partially due to the unavoidable difficulty of disentangling the relative contribution of these two factors in the context of clinical and epidemiological studies. This lack of knowledge limits our understanding of the neurobiological mechanisms of psychiatric symptoms, constraining the development of targeted therapeutic strategies and social programs to improve the quality of life of the patients. In this study, we tested a "double-hit" mouse model to study the interplay between a specific kind of early-life adverse experience and a specific genetic vulnerability in the emergence of central psychiatric traits. To do so, we used mice with heterozygous deletion of the CNTNAP2 gene. In the human population, homozygous mutation of CNTNAP2 is responsible for a severe neuropsychiatric disorder characterized by autistic-like symptoms, mental retardation, epilepsy and cortical dysplasia (Rodenas-Cuadrado et al., 2016). Knock-out mice lacking the CNTNAP2 gene (*Cntnap2*$^{-/-}$) successfully recapitulate this condition (Peñagarikano et al., 2011, 2015). To the contrary, current literature lacks a consensus on the specific association between CNTNAP2 heterozygous mutation and an exclusive diagnosis (Canali and Goutebroze, 2018; Ji et al., 2013; O'Dushlaine et al., 2011; Toma et al., 2018; Wang et al., 2010). People carrying heterozygous CNTNAP2 mutation present a phenotypic spectrum that

* Corresponding author. Istituto di Neuroscienze, Consiglio Nazionale delle Ricerche. Via G. Moruzzi, 56124, Pisa, PI, Italy.
** Corresponding author. Center for Mind/Brain Sciences, University of Trento. Piazza della Manifattura 1, 38068 Rovereto, TN, Italy.
E-mail addresses: gabriele.chelini@in.cnr.it (G. Chelini), yuri.bozzi@unitn.it (Y. Bozzi).
[1] Current affiliation: Istituto di Neuroscienze, Consiglio Nazionale delle Ricerche, Via G. Moruzzi, 56124, Pisa (PI), Italy.

https://doi.org/10.1016/j.ynstr.2025.100726
Received 4 March 2025; Received in revised form 9 April 2025; Accepted 17 April 2025
Available online 22 April 2025

ranges from neurotypical to autism spectrum (ASD) (Rodenas-Cuadrado et al., 2016), bipolar disorder (O'Dushlaine et al., 2011; Wang et al., 2010), and schizophrenia (O'Dushlaine et al., 2011; Wang et al., 2010). Importantly, according to current literature, rodents carrying the CNTNAP2 mutation (*Cntnap2*$^{+/-}$) do not display significant deviations from their wild-type (WT) littermates, from a behavioral standpoint (Peñagarikano et al., 2011; Scott et al., 2020). We reasoned that the phenotypic heterogeneity related to CNTNAP2 haploinsufficiency may arise as a consequence of the gene-environment interaction. A previous study explored this possibility by exposing *Cntnap2*$^{+/-}$ to a prenatal Poly-I:C maternal immune activation, resulting in the emergence of autistic-like behaviors in this model (Haddad et al., 2023). In this work we hypothesized that applying an early-life adverse experience to *Cntnap2*$^{+/-}$ mice may shape an alternative phenotypic trajectory, impacting core behavioral domain with transdiagnostic relevance such as stress and anxiety.

To test this hypothesis, we raised a group of *Cntnap2*$^{+/-}$ with limited bedding and nesting (LBN), a well-established paradigm to induce early-life stress in rodents (Walker et al., 2017). Previous studies show that WT mice raised in LBN show slight, but meaningful signs of altered stress and anxiety regulation, highly influenced by fundamental sex-differences (Brenhouse and Bath, 2019; Chelini et al., 2022; Manzano Nieves et al., 2020, 2023; Walker et al., 2017), which were partially replicated in our hands. Interestingly, these alterations were found in combination with signs of hypertrophy and gain-of-function in cellular, molecular and functional characteristics of brain areas involved in emotion regulation, such as the basolateral nucleus of the amygdala (BLA) and the prefrontal cortex (Brenhouse and Bath, 2019; Chelini et al., 2022; Guadagno et al., 2021; Manzano Nieves et al., 2020, 2023; Walker et al., 2017).

In this study, litters composed of both *Cntnap2*$^{+/+}$ and *Cntnap2*$^{+/-}$ raised in LBN (from this point onward defined as WT-LBN and HET-LBN, respectively) were compared with parallel litters of standard reared *Cntnap2*$^{+/+}$ and *Cntnap2*$^{+/-}$ (defined as WT-CTRL and HET-CTRL, respectively) to investigate the specific effect of the variables: gene, environment, sex, and their interactions. Mice were evaluated with a behavioral battery to assess multiple phenotypic domains: stress and anxiety, risk-taking, social interaction, repetitive behaviors, and context-based locomotor activity. Our results show that HET-LBN mice engage in excessive risk-taking behavior, ambivalent pattern of social interaction and increased locomotor activity in anxiogenic context. Conversely, we failed in detecting clear signs of autistic-like hallmarks such as clear deficits social interaction or motor stereotypies.

Finally, in HET-LBN mice, we provide evidence for synaptic hypertrophy and aberrant microglia morphology in BLA, suggesting a potential synaptic-driven mechanism governing the abnormalities in the affective behaviors resulting from the combination of *Cntnap2* haploinsufficiency and early-postnatal stress.

2. Materials and methods

2.1. Animals

All experimental procedures were performed in accordance with Italian and European directives (DL 26/2014, EU 63/2010) and were reviewed and approved by the University of Trento animal care committee and Italian Ministry of Health. Animals were housed in a 12h light/dark cycle with unrestricted access to food and water. All sacrifices for brain explant were performed under anesthesia and all efforts were made to minimize suffering. A total of 108 age-matched adult mice (weight 25–35 g), derived from a total of 19 litters (11 controls and 8 LBN), were used for the behavioral study. All mice were generated from our inbred *Cntnap2* colony with C57BL/6 background. Both males (M) and females (F) were used in the study.

Breeding strategy. To minimize the effect of confounding factors on the variables of interest (i.e. early-life stress and genotype), we adopted a standardized breeding strategy. Age-matched (postnatal age P = 150–160 days) *wild-type* females were crossed with heterozygous males, eliminating the effect of maternal age and genotype on parental care. The choice of only using wild-type female dams was driven by the necessity of excluding the possibility of confounding effects due to the interaction of maternal genotype with the LBN procedure. The first litter was discarded to exclude the consequences of first experience in maternal care. Only second-born litters were included in the study (Fig. 1A shows a schematic representation of the breeding strategy).

2.2. Limited bedding and nesting

The limited bedding and nesting paradigm was adapted from Walker et al. (2017). At postnatal day 4 (P4) the dam with the entire litter was moved to an experimental cage. The cage featured an aluminum mesh placed at 2.5 cm distance from the base and nestled material reduced to ¼ with respect to a standard cage. The mother with the full litter was returned to a standard breeding cage once the pups reached P11. Control litters were moved from standard cages to standard cages at the same time-points, to exclude the effect of experimental manipulation as a confounding factor. Both LBN mice and controls were weaned at postnatal day 21/22 and housed in standard cages with a single nestled square as an enrichment. Post-weaning, mice were group housed in cages of 2–5 subjects coming from the same litter (thus mixing wild-type and heterozygous individuals), sorted by sex. To avoid results inconsistencies in the behavioral assessment derived from the acute effects of home-cage social hierarchy (Karamihalev et al., 2020) mice were single housed 2-weeks prior to the beginning of the behavioral battery, thus balancing the experimental conditions across the entire cohort.

2.3. Behavioral battery

A specialized battery was designed including five well-established tests to assess both stress and anxiety domain as well as autistic-like behaviors. The battery lasted for 5 days, with a different test administered on each day (Fig. 1B). All mice were tested at 3 months of age. During the week prior to the beginning of the battery, animals were daily acclimated with the room and the experimenter for five consecutive days, including 1–2 min daily session of gentle handling. On test days, each mouse was acclimated with the experimental room for 20 min before the beginning of the test. All tests were performed in dim light (4 lux; with the obvious exception of the Light/Dark transition boxes) and recorded by an overhead camera secured above the apparatus. For all test, apart from the marble burying, mice were tracked using the software EthoVisionXT (Noldus, Wageningen, the Netherlands). The quantification of dependent variables was automatically provided by the features included in the EthoVisionXT. Dependent variables of interest and their acquisition settings were selected prior to the beginning of the first batch of experiments, based on their relevance with respect to each test, and kept consistent across the entire study. A full list of the outcome measures used in the study is summarized in Table 1. To investigate the time-dependencies of some behavioral traits, each test (except for the marble burying) was analyzed by splitting the total time of the test (10 min) in two separate trials (0–5 min/5–10 min). For behavioral testing, groups were composed as follow: WT-CTRL n = 34 (16 M/18 F); WT-LBN = 21 (7 M/14 F); HET-CTRL = 23 (11 M/12 F); HET-LBN = 30 (18 M/12 F). The whole study was conducted in a total of 11 technical/biological replicates. Each replicate comprised subjects coming from both LBN and standard reared cage, caring to balance sex and genotype in each batch.

Open field (OF). Mice were placed and let free to explore an open space in a squared arena (40 x 40 × 40 cm) for a total of 20 min while vide-recorded (Kraeuter et al., 2019). Only the results of the first 10-min are reported in this work as to match the timeframe of the other stress and anxiety tests.

Three-chamber test. The apparatus consisted of a plexiglass

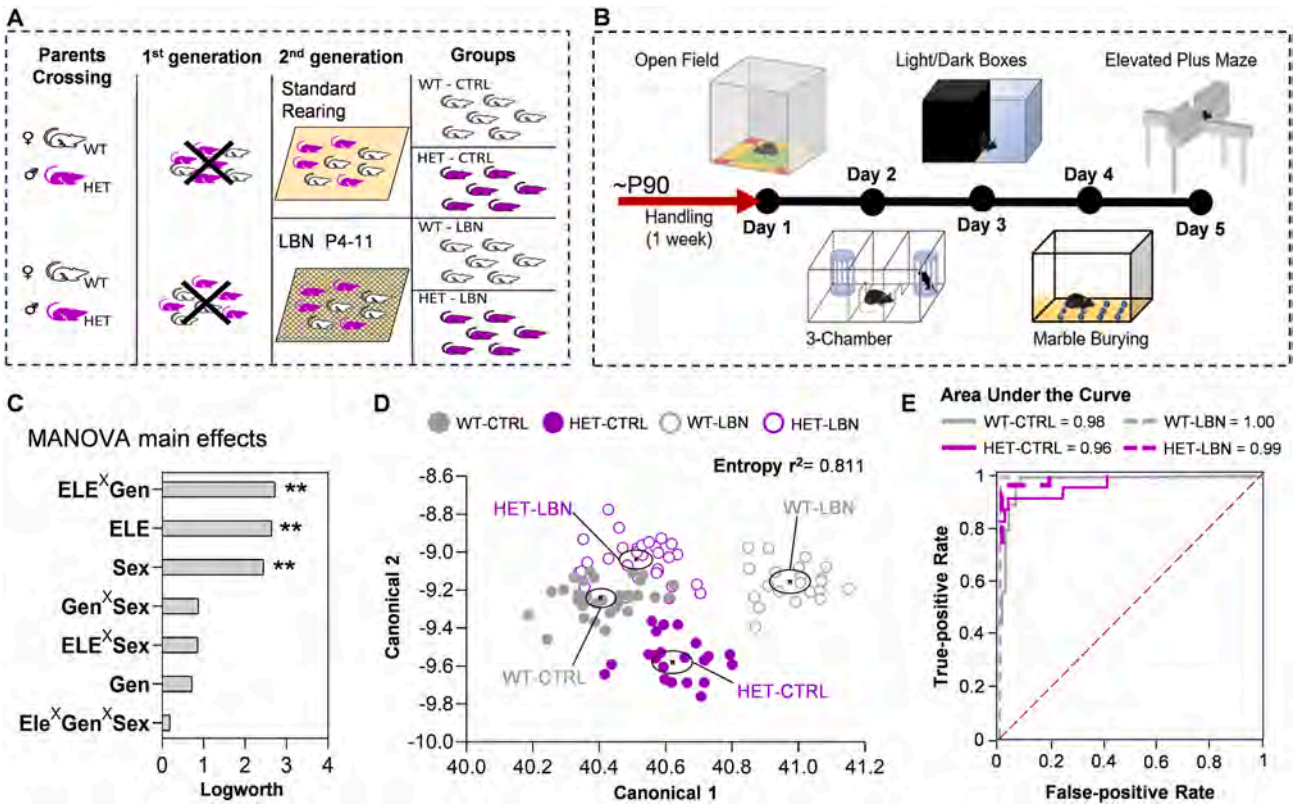

Fig. 1. Generation and assessment of the four of experimental groups revealed a main effect of gene-environment interplay in shaping the behavioral domain **(A)** Schematic representation of the breeding strategy for the generation of the experimental groups. **(B)** Outline of the behavioral battery used for the assessment of stress and anxiety and autistic-like behaviors. **(C)** MANOVA, using the output measure of the whole behavioral assessment, unraveled a significant effect of the Gene-environment interaction, followed by ELE and sex. **(D)** Centroid plot resulting from MANOVA analysis displaying the behavioral discrepancies between groups. **(E)** A discriminant algorithm predicts, with nearly perfect accuracy, the group identity of all subjects as testified by the ROC curve, confirming that the behavioral assessment successfully harnesses the phenotypic differences between the four experimental conditions. *p < 0.05/**p < 0.001/***p < 0.0001.

rectangular box (60 x 40 × 22 cm), each chamber (20 x 40 × 22 cm) having blacked colored external walls and transparent panels separating the 3 chambers (Kaidanovich-Beilin et al., 2011). Immediately after the open field test, always the day before the 3-chamber, mice were placed in the three-chamber apparatus and allowed to freely explore it for 20 min. On test day, mice were put in the apparatus and let free to navigate for the first 10 min (habituation phase). Then, the sociability test started by introducing one unfamiliar mouse (social target) placed into a wire cylindrical cage (20 cm in height, 10 cm bottom-diameter, 1 cm bars spaced) in one of the corners of one of the lateral chambers. The social target was an adult *wild-type* mouse (3–5 months old) derived from the same colony as the testing mice. The sex of the social target was matched with the sex of the testing mouse. An identical empty wire cage was placed in the equivalent corner of the opposite chamber. The test mouse was allowed to freely interact with the unfamiliar mouse or the empty cage for 10 min. No differences were found between the first and the second half of the 3-chamber test, thus we only present here the results for the total time of the test (10 min).

Ligh/Dark boxes (L/D). Mice were introduced into an arena (40 × 25 × 25 cm) split in two halves (chambers) separated by a black panel (Takao and Miyakawa, 2006). One half of the arena had the walls externally coated in black, fully shielding it from the light. The other half had transparent walls and a bright light source positioned nearby. A 5 × 8 door allowed the mice to freely transition between the two halves. Animals were allowed to freely move into the apparatus for a total of 10 min while videotaped.

Marble Burying. Five cm of standard mouse bedding were put in a standard rat cage (26 cm × 48 cm x 20 cm) and 16 standard glass toy marble were positioned in 4 rows equidistant from each other (Angoa-Pérez et al., 2013). Mice were let free to navigate the cage for 30 min while videotaped. For every 5 min of the test, a snapshot of the video was taken to quantify the number of marbles buried at that interval. 1 point was assigned to marble covered for more than 75 % of their visible surface; 0.5 points were assigned when a marble was buried for less than 75 %. No major informative differences were found in this test; thus, the results are only reported in the Supplementary Fig. 1.

Elevated Plus Maze (EPM). Mice were place at the center of a standard elevated plus maze apparatus, consisting of a two open arms (25 x 5 × 0.5 cm) across from each other and perpendicular to two closed arms (25 x 5 × 16 cm) and a center platform (5 x 5 × 0.5 cm) (Komada et al., 2008). Animals were allowed to freely move into the apparatus for a total of 10 min while videotaped.

For the integrated assessment of anxiety levels and exploratory behavior, all 3 partitioning of the apparatus were taken into account: the closed arm representing a safe zone with no exploratory activity; the center being the safe exploratory option and the open arm being the risky exploratory alternative. In this work, the EPM was exploited to highlight differences in risk-taking strategies across the four groups, as previously described (Bagheri et al., 2022; Florén Lind et al., 2023).

2.4. Definition of indexes used in the behavioral assessment

To disentangle the nuances of behavioral complexity in tests consisting on more than two forced choices (thus not the L/D and marble burying), we calculated a set of indexes that convey information about animal preferential choices. In each formula 'T' stands for "time", 'F' stands for "frequency".

OF. To assess the subject preference for a safe zone (corners), versus

Table 1
List of the outcome measures used in the behavioral assessment for each of the test.

TEST	Variable Name	Description
Open Field	OF Center - Freq	Frequency entries center of the arena
	OF-Center- Time	Time spent in the center of the arena
	OF Corner - Freq.	Frequency entries corners of the arena
	OF-Corner - Time	Time spent in the corners of the arena
	OF Velocity	Velocity
	OF Distance Traveled	Distance Traveled
	OF Moving Freq	Frequency animal start moving
	OF Moving Time	Time spent moving
	OF Immobile Freq	Frequency animal not moving
	OF Immobile Time	Time spent not moving
	OF Acceleration Max	Maximum acceleration
Light/Dark Boxes	L/D Latency Light	Latency to enter light chamber
	LD/5min - Freq. Light	Frequency entries in the light chamber
	LD/5min - Time Light	Time spent in the light chamber
	LD/5min - L/D Velocity	Velocity
	LD/5min - L/D Accel Max	Maximum acceleration
	LD/5min - Distance Traveled	Distance Traveled
	LD/5min - Immobile Freq	Frequency animal not moving
	LD/5min - Immobile Time	Time spent not moving
Elevated Plus Maze	EPM/5min - Freq Open	Frequency entries in the Open Arm
	EPM/5min - Time Open	Time spent Open Arm
	EPM/5min - Freq Closed	Frequency entries in the Closed Arm
	EPM/5min - Time Closed	Time spent Closed Arm
	EPM/5min - Freq. Center	Frequency entries in the Center
	EPM/5min - Time Center	Time spent Center
	EPM/5min – Freq. Mobile	Frequency animal start moving
	EPM/5min - Time Mobile	Time spent moving
	EPM/5min - Freq. Immobile	Frequency animal not moving
	EPM/5min - Time Immobile	Time spent not moving
3-Chamber Test	3C - Freq. Nose in Social Area	Frequency the animal is sniffing the social target
	3C - Time Nose in Social Area	Time spent sniffing the social target
	3C - Freq. Nose in Item Area	Frequency the animal is sniffing the object
	3C - Time Nose in Item Area	Time spent sniffing the object
	3C - Freq. Nose in Social Target	Frequency the animal is interacting with the social target
	3C - Time Nose in Social Target	Time spent interacting with the social target
	3C - Freq. Nose in Item Target	Frequency the animal is interacting with the object
	3C - Time Nose in Item Target	Time spent interacting with the object
	3C - Freq. in Social Chamber	Frequency entries in the social chamber
	3C - Time in Social Chamber	Time spent in social chamber
	3C - Freq. in Item Chamber	Frequency entries in the object chamber
	3C - Time in Item Chamber	Time spent in object chamber
	3C - Distance Traveled	Distance Traveled
	3C - Velocity	Velocity
	3C - Center Freq	Frequency entries in the center chamber
	3C - Center Time	Time spent in center chamber
Marble Burying	MB - Max Overtime	Maximum marble buried during the test

All these variables were used for the MANOVA and discriminant analysis.

an anxiogenic one (center of the arena) we used an index defined as: *Safety Preference Index = T Corners/(T Corners + T Center)*. The preference for arena borders against the center (thigmotaxis) was defined as:

Thigmotaxis = T Borders / (T Borders + T Center).

EPM. To assess the subject preference for a safe exploration (center of the maze) versus a dangerous alterntive (open arms) we used two indexes defined as: *Safe Exploration Index = F Center/(F Center + F Open Arms); Safe Exploration Index = T Center/(T Center + T Open Arms)*. The preference for safe areas (closed arms) versus anxiogenic ones (open arms) was defined as:

Safety Preference Index = F Closed Arms / (F Closed Arms + F Open Arms); Safety Preference Index = T Closed Arms / (T Closed Arms + Time Open Arms).

For all tests, the calculated indexes span from 0 to 1, where 1 represents complete preference for a safe choice while 0 represents complete preference for the risky choice.

The social preference was calculated using the formula: *Social Preference Index = T sniffing the mouse/(T sniffing the mouse + T sniffing the empty object)*.

2.5. Tissue processing and immunofluorescence

One month after the end of the behavioral battery, mice were deeply anesthetized with isoflurane and sacrificed by decapitation. Brains were excised and split in two halves. The right hemisphere was freshly dissected in multiple brain regions, snap-frozen in dry ice and preserved at −80° for future studies. The left hemisphere was washed in 0.1 % phosphate buffer saline (PBS) and post-fixed overnight in 4 % paraformaldehyde (PFA), switched to a cryoprotectant solution (80 % PBS, 20 % glycerol with 0.1 % sodium azide) and stored at 4 °C. Cryoprotected brains were sectioned on a vibratome (Leica, VT1200) at 40 μm thickness. Serial sections were collected in 24 separate compartments and stored at 4 °C in cryoprotectant solution.

Synapse study. Free-floating slices were rinsed three times in PBS (10 min each), then washed in PBS containing 0.2 % detergent (Triton-X, Fisher, AC215680010) for 30 min. Tissue sections were then incubated in blocking solution [2 % Bovine serum albumin (BSA), 1 % fetal bovine serum (FBS) in PBS] for 3 h and then transferred to primary antibody solution [2 % BSA, 1 % FBS, 1 to 1000 dilution of primary antibody (Rabbit anti-PSD95, Abcam, ab18258)] and incubated at room temperature for 24 h. Then, sections were rinsed three times in PBS (5 min each) and placed in a fluorophore-conjugated (Alexa Fluor™ Plus 488) secondary antibody solution [1:500 dilution of donkey anti-Rabbit secondary antibody (Thermo Fisher, AB_2762833) in PBS] for 24 h. Sections were then washed 5 min in PB, mounted on superfrost slides, dried for 1 h and coverslipped with fluorescent mounting medium (Southern biotech 0100–01).

Microglia study. Floating slices were permeabilized in 0.5 % Triton X-100 in PBS for 90min at RT, followed by incubation with blocking buffer (2 % BSA in permeabilization buffer) for 1h at RT. Primary antibodies were diluted in blocking buffer (Iba1, 1:1000, Wako cat no 019–19741; CD68, 1:400, Bio-Rad cat no MCA1957) and incubated overnight at 4 °C with mild agitation. Brain slices were then washed in PBS at RT for 3 times, 10 min per wash, and further incubated with Alexa Fluor Plus-labelled secondary antibodies (1:1000 in blocking buffer) for 2h at RT. After additional 3 washes in PBS, nuclei were stained for 10 min at RT with DAPI (1 μg/ml in PBS). Finally, slices were mounted on microscope slides using Mowiol 4–88 (Sigma Aldrich, cat no 81381). For both studies, slides were stored at 4 °C in the dark until use.

For immunostaining, 8 subjects were chosen from each group, balancing males and females (4 M and 4 F per group). The same subjects

were used in both synapse and microglia studies, selecting slices with immediate stereological proximity.

2.6. Confocal microscopy and image analysis

Synapse study. A confocal laser scanning microscope Leica TCS-SP8, equipped with a HC PL APO 40× objective and interfaced with Leica "LAS-X" software was used. Images were recorded at a resolution of 1024 pixels square, 400 Hz scan speed with a zoom factor of ×5 to maximize puncta visualization. Excitation/emission wavelengths were: 490/520 for Alexa-488 fluorophore. Acquisition parameters were set during the first acquisition and kept consistent for all the images. For each subject, six size-matched (36 × 36 μm) z-stack images were acquired from the BLA using a pseudo-random strategy, caring to exclude cell bodies from the images and focusing exclusively on the dendritic neuropil. Each stack spanned for a total of 10 μm thickness, with a step-size of 0.5 μm. The maximum intensity projection for each z-stack was post-processed using the "subtract background" and "despeckle" features within the imageJ software (NIH, USA) (Schneider et al., 2012) and quantified with the "3D object counter" plug-in. Postprocessing and detection settings were kept consistent across all images.

Microglia study. Acquisitions were taken at a Stellaris 5 confocal microscope (Leica), with a 63× objective and digital zoom of 1 (Z-stack, step size 0.3 μm). Identical imaging settings and resolution (1024 × 1024 pixels) were maintained across all the tested conditions for each experiment. Microglia morphometry and engulfment analyses were carried out using the Imaris software (Bitplane). 3D reconstruction was performed with the built-in "Surface" function by applying the same thresholds across all the tested conditions. All entire microglia cells per field of view were reconstructed and analyzed.

2.7. Statistical analysis

All statistics were computed using the software JMP-pro17. The discriminant analysis algorithm included all the relevant metrics obtained in the behavioral assessment (Table 1). For the behavioral studies, a 3 × 3 multiple regression model was applied to test for the main effects of covariates *early-life experience* (ELE), *genotype* (Gen) and *sex*, and their interactions. Whenever the variable sex was found not significant, it was excluded from the statistical analysis. When the variable sex was found to significantly impact the results, but in equivalent degree for all 4 experimental groups, a multiple regression model was applied to exclude the effect of this covariate from the data. No major effect of the interaction between sex and other variables was found in most of the studies, thus the results of multiple comparisons reported in the main text do not report sex differences. The only test showing a meaningful sex-bias was the L/D boxes, for which we report the sex-dependent multiple comparisons in Supplementary Fig. 3. All multiple comparisons were calculated using Tuckey's correction. To compare the first half of each test (0–5 min) with the second half (from 5 to 10 min) we used a 2-way mixed model ANOVA; in this case, multiple comparisons were calculated using Sidak's correction.

The multiple regression model to eliminate the effect of risk-taking from the results of the social interaction was performed as follow: the regression coefficients (intercept "α" and slope "β") were calculated, for each group, using the "Frequency open arm in the 5_10 min interval" as explanatory and "Sniffing time" as response variables. For each subject, the predicted impact of risk-taking was calculated by multiplying the value "Frequency open Arm 5_10 min" for the β coefficients. Finally, the resulting value was subtracted from the variable "Sniffing Time".

$$Corrected\ Sniffing\ time = Sniffing\ time - (Freq.\ Open\ Arm\ 5\_10\ min * \beta)$$

For the stratification of social-behavioral profiles we used a principal component analysis that led us to select three major principal components explaining most (90 % of the variance), as shown in Fig. 5A. These three leading components were used to perform an iterative *k-mean* clustering testing from 1 and up to N (=108) models. Then, using the average distance from centroids for all 108 models, we selected the number of k that offered the best reduction in the within-cluster sum of squares (elbow method, displayed in Fig. 5A (Thorndike, 1953) obtaining a number of cluster k = 4. An extensive report of the statistical analysis is summarized in Supplementary file n.1.

3. Results

3.1. Early-life adversity determines distinct behavioral phenotypes based on genetic background

First, we sought to determine which of the independent variables (early-life experience, genotype, sex) had a primary effect on the behavioral domain by using a multivariate analysis of variance that included the outcome measures from the whole behavioral battery (Table 1, Fig. 1B). This analysis revealed a primary effect of the interaction between genetic background and early-life experience (ELE), followed by an identical significant impact of both ELE and sex (Fig. 1C). By consequence, the related discriminant analysis successfully classified the four experimental group into four distinct subpopulations (Fig. 1D), with virtually perfect accuracy (Fig. 1E).

Our findings establish that the application of LBN during early postnatal age shape the behavioral trajectories based on genetic predisposition, giving rise to four distinct phenotypic landscapes.

3.2. Cntnap2 haploinsufficiency mitigates LBN-derived anxiogenic behavior in the open field

As a first step in the behavioral assessment, we looked for signs of generalized anxiety in the open field (Fig. 2A). At the 0–5 min interval, we highlighted a main effect of the ELE, which resulted in a significant increase in the safety preference index in both WT-LBN and HET-LBN groups compared to WT-CTRL (Fig. 2B). This was accompanied by a significant increase in the time spent in the corners, specific for the WT-LBN group (Fig. 2C). No group difference was found in the 5–10 min interval, while the main effect of ELE persisted (Fig. 2D). These findings suggest that early exposure to scarcity-adversity is sufficient to exacerbate an anxiogenic phenotype, but this effect is partially mitigated by *Cntnap2* haploinsufficiency. Additionally, we used multiple motility descriptors to assess potential discrepancies in the locomotor activity. We found that none of the parameters analyzed (velocity, distance traveled, time and frequency mobile and immobile) were affected by the experimental conditions (Fig. 2E, F and Supplementary Fig. 2). This establishes that neither haploinsufficiency of *Cntnap2* nor postnatal LBN negatively impact motor abilities nor exacerbate hyperactive behavior in mice.

3.3. Both LBN and Cntnap2 heterozygous mutation independently result in a hyperactive phenotype in the L/D transition test

To further explore the effect of the LBN onto anxiogenic behavior, we challenged the four experimental groups in the L/D test, evaluating their risk-assessment strategy in a condition of perceived danger (i.e. light chamber, Fig. 2G). In this setting, no differences were found between the four experimental groups in the time spent in the light chamber, at neither time-point (Fig. 2H). However, during the first 5 min only, we observed a main effect of the variable sex that was primarily driven by an increase in the time spent in light displayed by the males of the WT-LBN group, compared to females (Supplementary Fig. 3A). This sex-bias was abolished in the HET-LBN (Supplementary Fig. 3B). Consistently, WT-LBN males showed to cover more distance during their exploratory activity in the light chamber (Supplementary. 3C and D). This finding confirms a previous work showing that LBN defines male-specific behavioral deviations in WT animals (Reshetnikov et al., 2021). However, by looking at the locomotor activity, we found a striking effect of

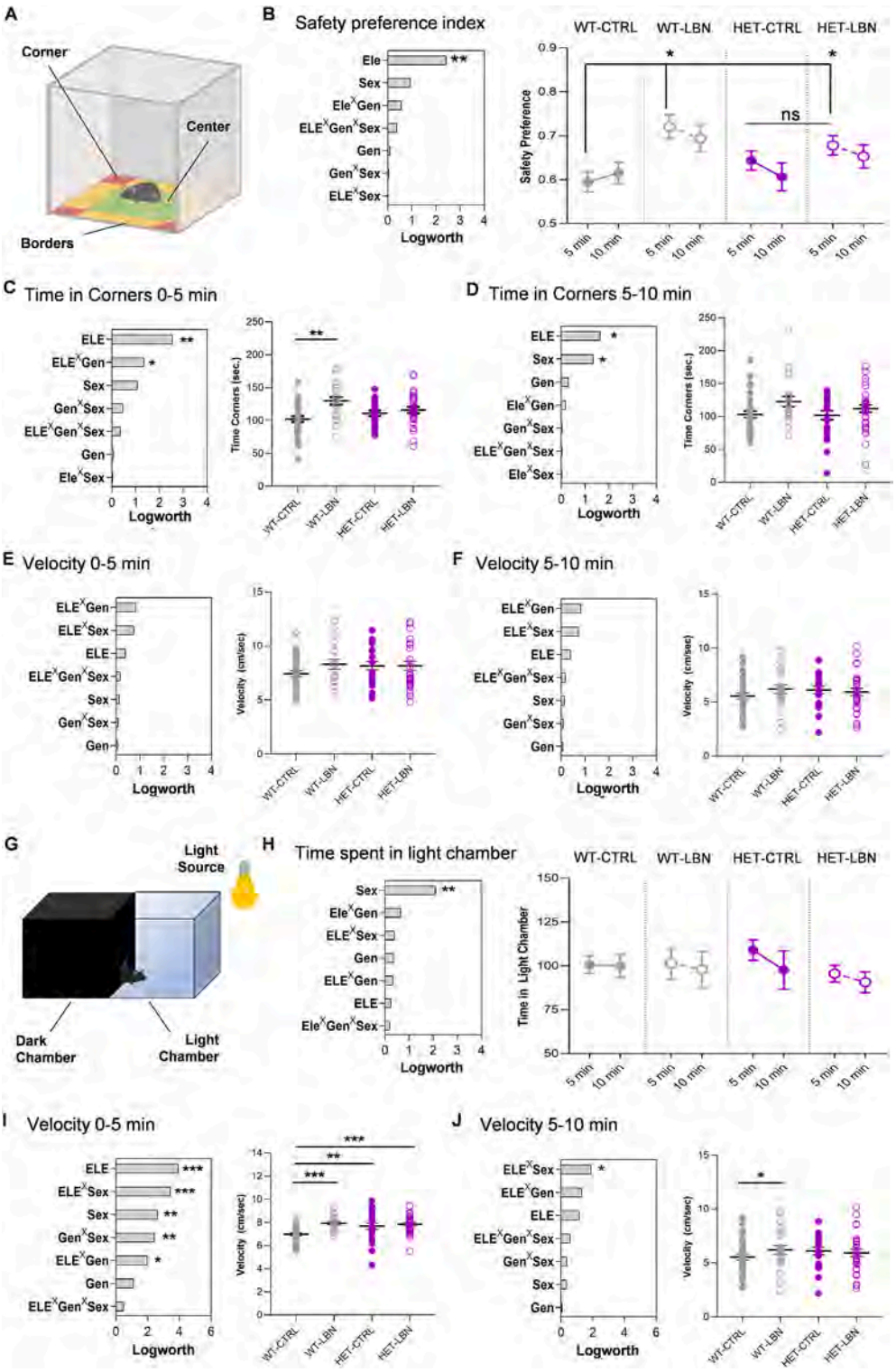

Fig. 2. LBN induces anxiogenic behaviors that are mitigated by *Cntnap2* haploinsufficiency **(A)** Graphical depiction of the Open Field arena and its partitions. **(B–F)** Left panels: charts summarizing the quantification of the main effect of the covariates included in the model; Right charts: depict the results of multiple comparisons for the given outcome measure. **(B)** A main effect of ELE determines a preference for the safe areas of the OF arena (corners) in both WT and HET-LBN groups, specifically during the first 5 min of the test. **(C)** During the first 5 min of the test, WT-LBN spend significantly more time in the corners compared to WT-CTRL, highlighting a main effect of both early-life experience (ELE) and the interaction between ELE and genotype (ELExGen). **(D)** A main effect of the ELE persists during the 5–10 min interval, but group differences are abolished. **(E, F)** No differences in the velocity indicates that neither ELS nor CNTNAP2 mutation have an impact on the locomotor activity. **(G)** Graphical depiction of the L/D arena and its partitions. **(H)** A remarkable effect of sex was found in the time spent in the light chamber, but no impact of either ELE or Genotype. **(I)** Both ELE and Genotype, as well as sex have a significant impact on the mice velocity in the light chamber during the first 5 min of the L/D test, resulting in a significant increase in all groups compared to WT-CTRL. **(J)** Only WT-LBN group maintain significantly higher speed in the second half of the test. See Fig. S2 for further details on sex differences. ELE = early-life experience; Gen = genotype; ^{X} indicates interaction. *p < 0.05/ **p < 0.001/***p < 0.0001.

both ELE and genotype onto the velocity within the light chamber, showing that all 3 experimental groups are statistically different from WT-CTRL (Fig. 2I) during the first 5 min of the test. Only the WT-LBN group showed a protracted change in the 5–10 min interval (Fig. 2J). Altogether these findings suggest that, when mice are provided with the option of exploring an aversive environment, both LBN and *Cntnap2* haploinsufficiency determines a severe hyper-active behavior, but only WT-males express a drastic change in their risk-assessment strategies. This confirms the results of the OF, showing that *Cntnap2* heterozygous mutation partially prevents the negative consequence of early-postnatal stress.

3.4. Early-life stress exacerbates perseverative risk-taking behavior in *Cntnap2*$^{+/-}$ mice

To further understand potential changes in risk-assessment strategies, we tested the four groups in the elevated plus maze (EPM). In this test we evaluated the mice tendency to risk-taking (walking in the open arm) against their natural predisposition to explore the surroundings from the center of the maze as an indicator of innate curiosity (Fig. 3A). We found that WT-CTRL mice display a drastic increase in the safe exploration index between the first and second half of the test, prioritizing a safe choice over a dangerous one, after an initial risk-assessment. This trend is preserved in both WT-LBN and HET-CTRL (although to a lesser degree in this latter group), but completely abolished in HET-LBN mice, highlighting a main effect of the gene × environment interaction (Fig. 3B and Supplementary Fig. 4B). These data are determined by an increase in both the frequency and the total time HET-LBN mice spend in the open arms of the maze compared to WT-CTRL during the sec half of the experimental session (Fig. 3C–E and S4C-D).

This finding suggests that, irrespectively from their early-life experience, mice possess an innate ability of tuning their behavior to privilege a safe choice against a potentially dangerous alternative. This ability is dampened by *Cntnap2* haploinsufficiency and exacerbates in a perseverative risk-taking behavior when *Cntnap2*$^{+/-}$ mice are raised in LBN. Finally, we discovered a main effect of the ELE on the locomotor activity during the first 5 min (Fig. 3F and G), with a subtle increase affecting both WT-LBN and HET-LBN mice, which corroborates our previous finding in the L/D test.

3.5. Successful social interaction in LBN-raised *Cntnap2*$^{+/-}$ correlates with their risk-taking behavior

Then, we assessed the social preference of the four groups using a classical 3-chamber test (Fig. 4A). At first, no main effect of variables sex, ELE or genotype, nor group differences could be appreciated, at neither time-points (Fig. 4B). All groups showed similar time spent sniffing the social target (Fig. 4C) as well as successful social preference (index above 0.5, Fig. 4D). Then, we asked whether any of the changes in anxiety regulation might play a role in the outcome of the social interaction by correlating the time spent sniffing the social target with all parameters extrapolated in the stress and anxiety evaluation (Figs. 2 and 3). Interestingly, the only positive association between affective state and social behavior was found in the HET-LBN group, where both the time and frequency of exposure to the open arm of the EPM significantly correlated with the time sniffing the conspecific (Fig. 4E).

Thus, we hypothesized that, for *Cntnap2*$^{+/-}$ mice raised in LBN, successful social interaction might be contingent on their willingness to take a risk. To verify this hypothesis, on the basis of our data, we used a multiple regression model to exclude the portion of variance explained by risk-taking (i.e. the variable "frequency open arm") from the results of the social interaction (i.e. variable "sniffing time" (Fig. 4F). Doing so, we found a main effect of the variable ELE in reducing the sniffing time, primarily derived by a significant reduction affecting the HET-LBN group compared to both WT- and HET-CTRL (Fig. 4G). This reduction resulted in the loss of the social preference in the HET-LBN group selectively (Fig. 4H). Importantly, no differences in the basic locomotor activity were detected during the habituation phase of the sociability test nor in the time investigating the inanimate object and neither of these parameters showed significant association with the risk-taking quantified in the EPM (Supplementary Fig. 5), putatively excluding an impact of the affective domain in basic locomotion or exploratory drive in the 3-chamber. These findings suggest that an intrusion of anxiety may alter the social-behavioral pattern in HET-LBN mice.

3.6. Alternative social-behavioral pattern highlights a larger proportion of HET-LBN mice lacking social preference

We then reasoned that if the anxiety domain interacts with the social strategies in HET-LBN mice this may give rise to an alternative pattern of social interaction. To test this hypothesis, we stratified our dataset according to the social parameters obtained with the 3-chamber test, using principal component analysis (PCA) followed by unsupervised clustering (Fig. 5A). Doing so, we identified four distinct modalities of social interaction that we named sociophenotypes (SPs) (Fig. 5B). The difference in social-behavioral parameters across SPs are summarized in Fig. 5C. Using the social preference index we then classified the four SPs in hypersocial (SP1), asocial (SP2), moderately social (SP3) and normosocial (SP4), (Fig. 5D). We notice that, in the HET-LBN group, the mildly social SP3 was nearly abolished, replaced by a larger percentage of the asocial SP2 (Fig. 5E). The similarity between HET-LBN and SP2 was further confirmed by multiple correspondence analysis, showing that these two groups segregate in close proximity, and isolated from all the others (Fig. 5F). To verify whether these abnormalities in social behavior may be linked to altered emotion regulation in the HET-LBN group, we then analyzed the safety exploration index across the four SPs and found no differences between the groups (Fig. 5G). This confirms that the group stratification obtained within the social domain does not overlap with underlying discrepancies in stress and anxiety. However, by splitting the HET-LBN group based on their successful social-behavioral strategy, we found that mice that belong to SP2 (socially impaired) are indistinguishable from other groups for the level of risk-taking measured in the EPM (Fig. 5H). Conversely, mice that showed a successful social preference (Sp1, 3, 4) displayed the same increase in risk-taking as shown in Fig. 3 (Fig. 5I). We conclude that, while not impaired in their social-behavioral skills, HET-LBN mice are more likely to express extreme gain or loss of function in their levels of social interaction, and that this condition may be consequence of their altered affective state.

3.7. Early-life stress forces excitatory synapses hypertrophy in the BLA

Then we hypothesized that the behavioral rigidity displayed by HET-LBN mice in the EPM may be linked to deficient synaptic turnover in a brain area dedicated to emotional processing. To investigate this possibility, we assessed the density and the size of PSD95-positive punctate in the BLA (Fig. 6A). We observed a close-to-significance effect of the variable ELE in both parameters (Fig. 6B and C). To get a better understanding of the impact of the LBN onto synaptic phenotype we analyzed the frequency distribution of the sizes of all the PSD95 puncta size identified. We found that, within each genotype, there is a significant shift of the distribution toward an increase in the percentage of larger post-synaptic densities (Fig. 6D and E). Thus, we sorted the PSD95-puncta into three size-based categories (small: from 30 to 70 voxels, medium: from 71 to 110 voxels and large from 111 to 150 voxels) and calculated the ratio between the number of puncta of each category against both of the others (Fig. 6F–H). We found no difference in the ratio between small-to-medium sized puncta (Fig. 6F). Conversely, a significant reduction in both the small-to-large as well as the medium-to-large ratios was found in both LBN groups (Fig. 6G and H). Additionally, the medium-to-large ratio was significantly decrease in the HET-LBN group compared to HET-CTRL (Fig. 6H). Finally, we

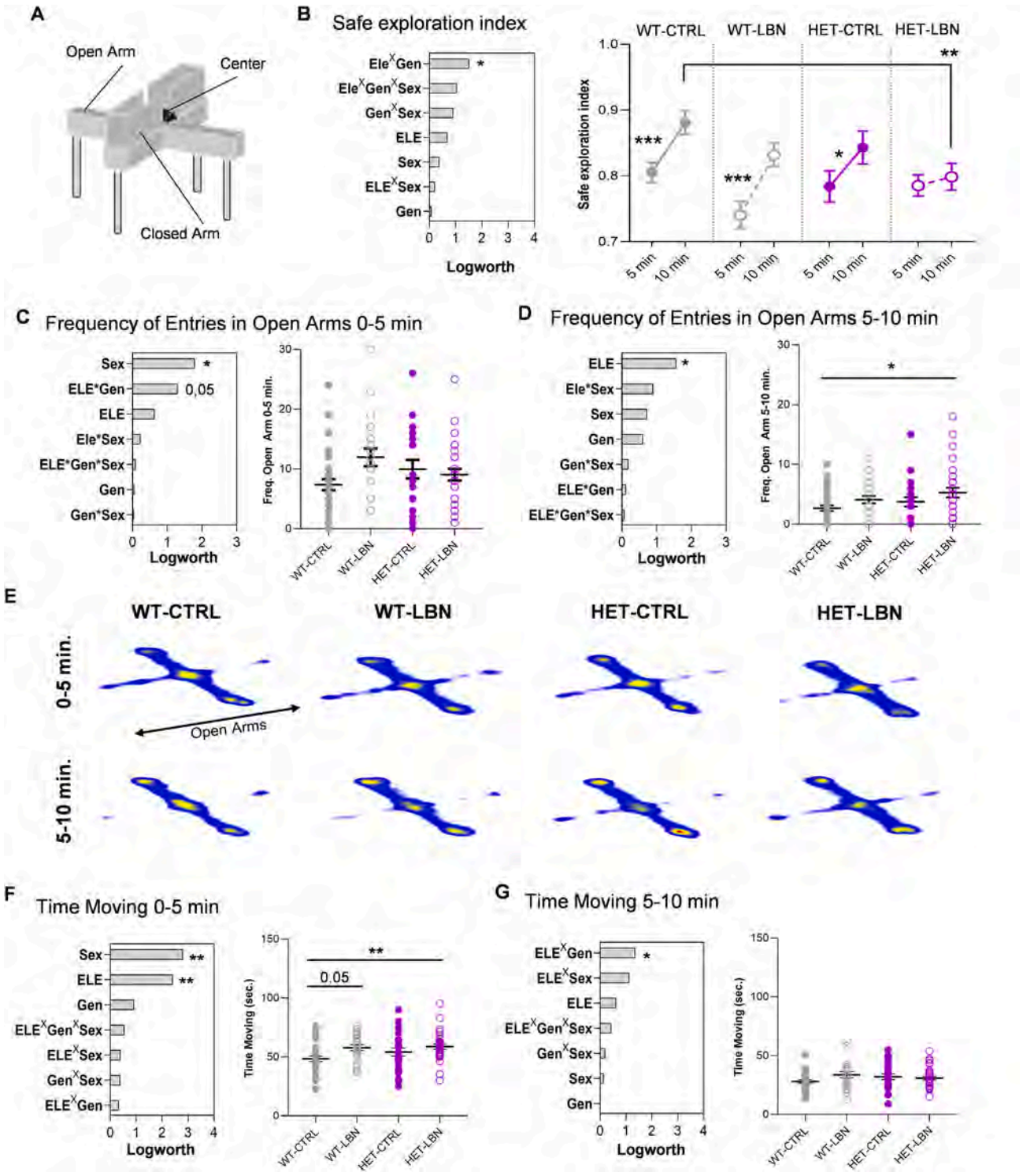

Fig. 3. HET-LBN mice display a perseverative risk-taking behavior in the EPM. **(A)** Graphical depiction of the elevated plus maze and its partitions. **(B-D, F, G)** Left panels summarize the quantification of the main effect of the covariates included in the model. Right charts depict the results of multiple comparisons for the given outcome measure. **(B)** A main effect of the interaction ELE^{X}Gen affects the mice preference for a safe area (center) versus a dangerous one (open arms); during the second half of the test, the safe exploration index increases in WT-CTRL, WT-LBN and HET-CTRL, but not in HET-LBN, resulting in a significant difference with WT-CTRL. **(C)** During the first 5 min, the frequency of entries into the open arm does not change in neither of the groups and only a shared effect of Sex is significantly explaining the model. **(D)** During the 5–10 min interval, a main effect of the variable ELE is explained by a significant increase in the frequency of entries in the open arm specific for the HET-LBN group compared to WT-CTRL. **(E)** Representative heatmaps depicting mice activity at both the time-points of the test; note how LBN exposure to the open arm persists beyond the first 5 min. **(F)** A main effect of LBN was found in the time moving in the maze for the 0–5 min interval, due to a slight increase in motility in WT-LBN and a large increase in HET-LBN. **(G)** Group differences in the motility state are abolished in the second half of the test, while a small effect of the interaction ELE^{X}Gen emerge.

ELE = early-life experience; Gen = genotype; ^{X} indicates interaction. *p < 0.05.

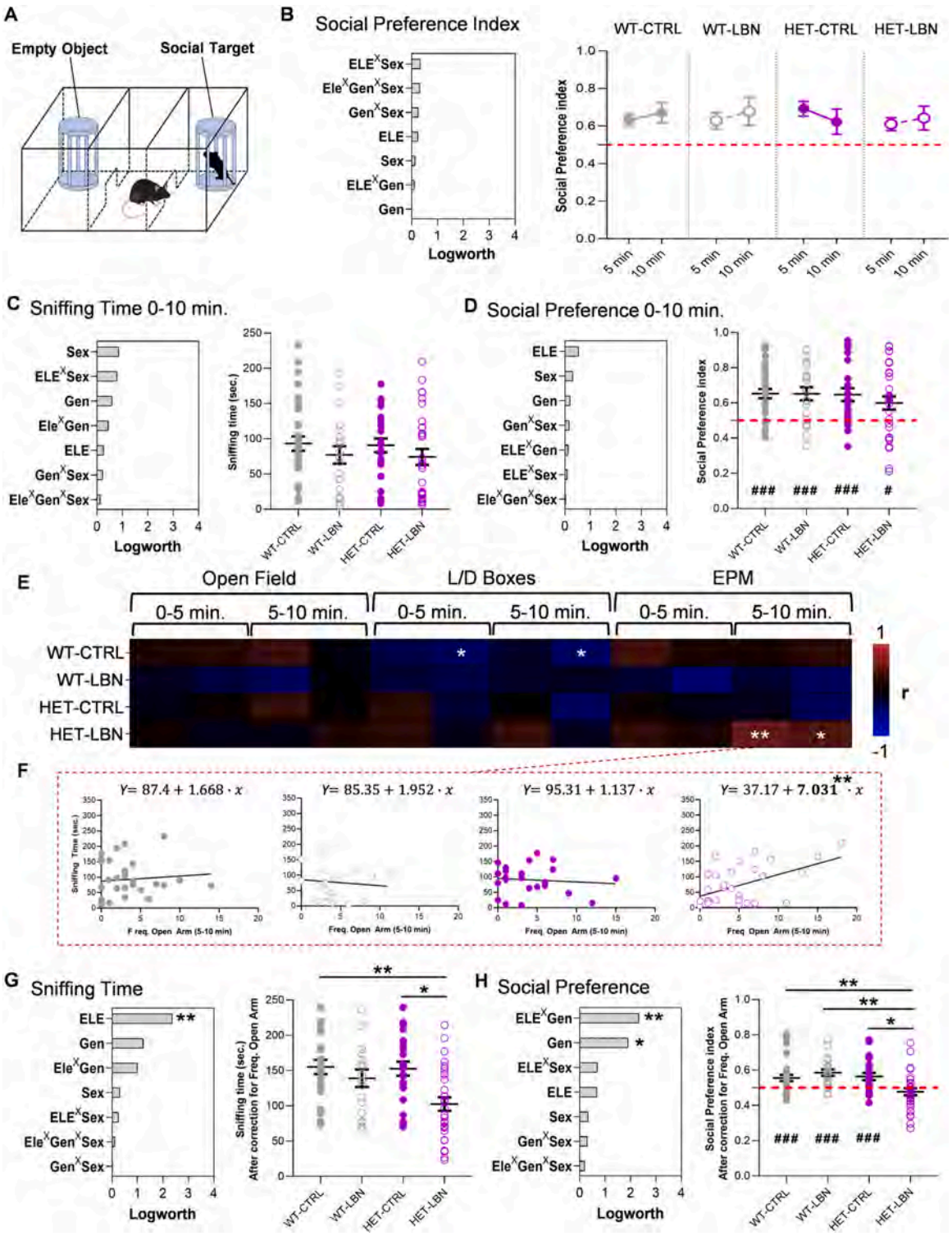

Fig. 4. Successful social interaction correlates with increased risk-taking in Cntnap2$^{+/-}$ raised in LBN. **(A)** Graphical depiction of the 3-chamber arena configuration. **B-D, G, H)** Left panels: charts summarizing the quantification of the main effect of the covariates included in the model; Right charts: depict the results of multiple comparisons for the given outcome measure. **(B)** Neither of the four groups display deficient social preference, at neither time-point. **(C–D)** Neither the time sniffing the co-specific **(C)** nor the social preference **(D)** are impacted by experimental conditions. **(E)** Correlation matrix between the time spent sniffing the social target and the outcome measures obtained in the stress and anxiety assessment. **(F)** Regression plot showing the linear relationship between the time spent sniffing the social target and the frequency of entries into the open arm. The regression coefficients were only significant in the HET-LBN group (WT-CTRL p = 0.618, WT-LBN p = 0.679, HET-CTRL p = 0.665, HET-LBN p = 0.004). **(G, H)** Results of the 3-chamber test after correcting the data for the effect of risk-taking behavior: **(G)** A main effect of the variable ELE results in HET-LBN mice spending less time sniffing the social target compared to both WT- and HET-CTRLs; **(H)** By consequence, HET-LBN display a lack of social preference due to a main effect of the ELE*Gen interaction.
ELE = early-life experience; Gen = genotype; ^{X} indicates interaction.
*p < 0.05/**p < 0.001/***p < 0.0001/# indicates social preference significantly different than chance: 0.5.

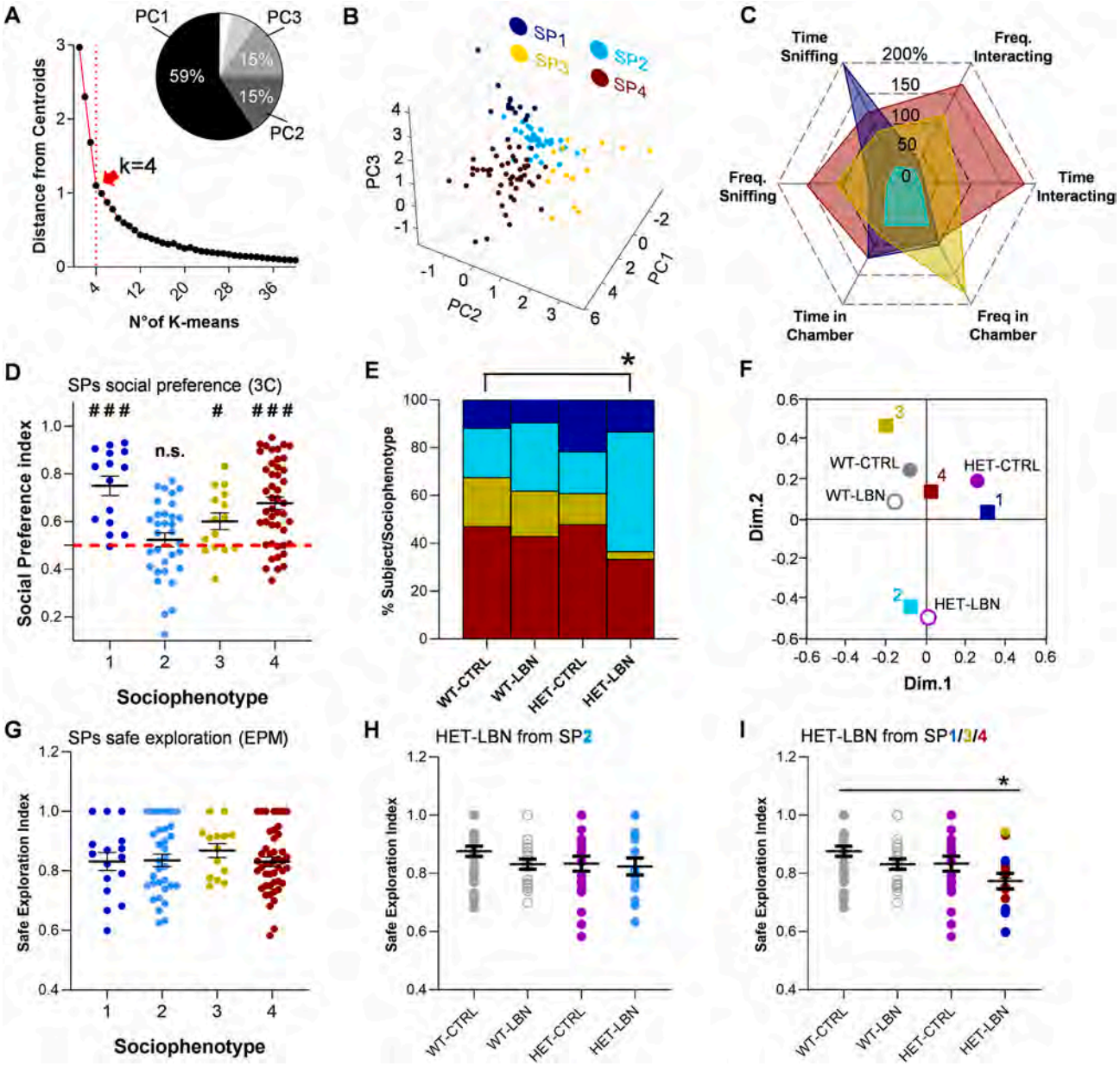

Fig. 5. Stratification of social-behavioral strategies suggests that HET-LBN mice are more likely to express deficits in social preference **(A)** Iterative *k-mean* clustering using the elbow method determined the presence of four distinct sociophenotypes (SPs); the pie chart shows the relative weight of each PC in explaining the variance. **(B)** 3D scatter plot showing the separation of the four SPs. **(C)** Radar plot displaying the differences in the social-behavioral strategies across the four SPs. (for each measure, data are normalized as the % change from the wholesome group mean). **(D)** SP2 is the only subcategory lacking a social preference. **(E)** Graphical depiction of the frequency distribution (%) of the SPs within each of the four experimental groups; note that SP2 is over-represented in the HET-LBN group, making it significantly divergent from WT-CTRL. **(F)** Multiple correspondence analysis confirms the overlap between SP2 and HET-LBN group. **(G)** SPs do not show any difference in the safety preference during the EPM. **(H, I)** By splitting the HET-LBN group based on their success in social interaction we found that: **(H)** mice belonging to the socially impaired SP2 do not show any alteration in their exploratory preference compared to other groups. **(I)** Conversely, mice from the socially successful SP1/3/4 display reduced preference for the safe option.
*$p < 0.05$/# indicates social preference significantly different than chance: 0.5.

discovered that the size of PSD95 puncta significantly, and exclusively, correlates with the safety preference index in the second half of the EPM (Fig. 6I). Specifically, the percentage of smaller puncta positively correlates with a preference for safety (Fig. 6J) while the percentage of medium and larger puncta associates with reduced preference for safety (Fig. 6K and L). Altogether these findings suggest that an early-life adverse experience promotes a decrease in the number of smaller synapses in favor of larger ones. This phenotype is intensified in *Cntnap2*$^{+/-}$ mice raised in LBN and may contribute to their maladaptive risk-taking behavior observed in the EPM.

3.8. Cntnap2 haploinsufficiency determines a vulnerability state in microglia that exacerbate in a hypertrophic phenotype after LBN

We then asked whether synaptic alterations in the BLA may be associated with microglia abnormalities. Microglia are emerging as key players in brain pathologies, including neurodevelopmental and neuropsychiatric disorders (Lukens and Eyo, 2022; Mondelli et al., 2017; Rahimian et al., 2021). Notably, microglial impairments are often associated with abnormal synapse density and function, leading to behavioral alterations in sociability, cognition and anxiety (Filipello

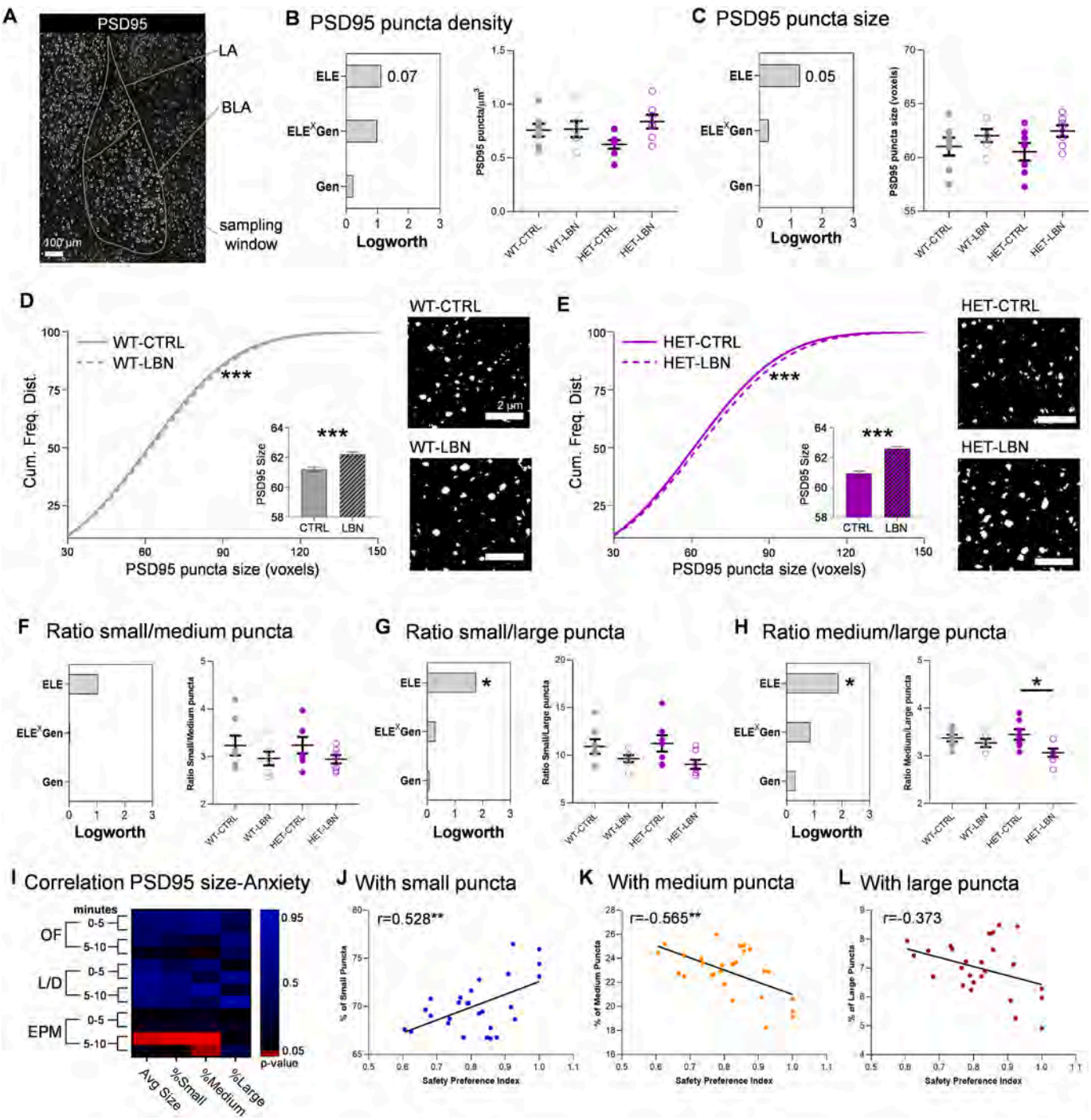

Fig. 6. LBN promotes synaptic hypertrophy in BLA: **(A)** Confocal photomicrograph of the basolateral amygdala (BLA) showing the location of sampling windows used for the analysis of PSD95 puncta. **(B, C, F-H)** Left panels summarize the quantification of the main effect of the covariates included in the model. Right charts depict the results of multiple comparisons for the given outcome measure. **(B, C)** A close-to-significant effect of ELE was found in both the density **(B)** and size **(C)** of PSD95 puncta. **(D, E)** Analysis of the relative frequency distribution of the puncta size revealed a significant shift in favor of larger puncta in both WT-LBN and HET-LBN groups compared to their respective WT-CTRL and HET-CTRL. **(F)** Ratio between small and medium puncta size is unaffected by the experimental conditions. **(G)** The ratio between small and large puncta is significantly affected by ELE, but does not result in group differences. **(H)** The ratio between medium and large puncta is significantly affected by ELE, with a stronger effect displayed in HET-LBN, significantly diverging from HET-CTRL. **(I)** The size of PSD95-puncta selectively correlates with the safety preference index during the 5–10 min interval of the EPM. **(J)** The percentage of smaller-sized puncta positively correlates with the safety preference while **(K)** the percentage of medium-sized puncta is negatively correlated. **(L)** Weak negative correlation between the percentage of larger spines and safety preference ($p = 0.05$).
ELE = early-life experience; Gen = genotype; ^{X} indicates interaction. *$p < 0.05$/**$p < 0.001$/***$p < 0.0001$.

et al., 2018; Monsorno et al., 2023; Zhan et al., 2014). We stained for IBA1 and CD68 to visualize and analyze microglial morphology and phagolysosomes, respectively (Fig. 7A and B). Morphometric analysis on three-dimensional cell reconstruction, revealed that WT-LBN and HET-CTRL microglia did not present any alteration compared to WT-CTRL, whereas HET-LBN microglia displayed almost a two-fold increase in volume (Fig. 7B–D). Consistently, we also found that the number and total volume occupied by $CD68^{+}$ structures were unchanged in WT-LBN and HET-CTRL microglia compared to WT-CTRL, but significantly higher in HET-LBN (Fig. 7B and E, Supplementary Fig. 5A). Conversely, the average volume of phagolysosomes was increased in HET mice, with a significant genotype effect (Fig. 7F). Next, we asked whether the higher content of CD68 particles per cell in HET-LBN could be just a mere consequence of microglial hypertrophy. When normalizing the number and volume of CD68 particles taking into account the microglial volume, we observed an increased CD68 content only in HET-CTRL, while this effect was absent in HET-LBN (Supplementary Fig. 5B–C).

Overall, these data suggest that the *Cntnap2* haploinsufficiency alone is not sufficient to affect microglial morphology, but that exposure to postnatal LBN is required to observe alterations in these cells. On the other hand, the phagolysosomal compartment is affected in control *Cntnap2*$^{+/-}$ mice, and the interaction with LBN dampens these alterations.

4. Discussion

In this study we combined a genetic vulnerability to neuropsychiatric disorders (*Cntnap2* heterozygosis) with an early-life stressful event to investigate the interplay between environmental stress and genetic predisposition in the emergence of transdiagnostic psychiatric hallmarks. First, we established that early-life adversity biases behavioral trajectories based on genetic predisposition, as testified by the significant effect of the ELE-genotype interaction in the MANOVA, and supported by the cohort stratification obtained with the discriminant analysis (Fig. 1). Then, looking at the specific outcome of each test, we discovered that both WT-LBN and HET-LBN groups displayed increased anxiety levels during the initial phase of the open field compared to WT-CTRL (Fig. 2). However, exclusively the *Cntnap2*$^{+/-}$ mice raised in LBN expressed an excessive risk-taking behavior (Bagheri et al., 2022; Florén Lind et al., 2023) by persistently walking into the open arm of the EPM, rather than using the center of the maze as a safe exploratory outpost (Fig. 3). We further noticed that HET-LBN animals are more likely to express behavioral strategies characterized by extreme levels of either positive or negative interaction, putatively depending on their affective state (Figs. 4 and 5). We propose that altered stress and anxiety regulation biases the social-behavioral domain in HET-LBN, determining an ambivalent pattern of hyper- or hypo-sociability. Finally, both in the L/D and EPM we noticed an increase in the locomotor activity for the HET-LBN group that only in the L/D was shared with other groups (HET-CTRL and WT-LBN). Altogether, these observations suggests that early-life adverse experience exerts a qualitative impact on the behavioral expression, depending on the genotype of the subjects, rather than linearly increasing, or decreasing, complex and multifaceted domains such as stress, anxiety and sociability.

To recapitulate, our study shows that *Cntnap2*$^{+/-}$ mice raised with LBN are characterized by: i) Increase risk-taking behavior (in the EPM), ii) affective-driven abnormalities in social interaction (3-chamber test), and iii) increased context-dependent locomotor activity (EPM and L/D boxes). Reasoning on this outcome in combination with *Cntnap2*-related conditions, we noticed some similarities with the DSM-5 criteria for bipolar disorder (American Psychiatric Association, 2022), which consist in: i) excessive involvement in activities that have a high potential for painful consequences, ii) sufficiently severe mood disturbance to impact on social functioning, iii) increased psychomotor agitation. On the other hand, we did not highlight significant disruption of sociability, nor signs of motor stereotypies, thus excluding the presence of clear autistic-like phenotype (Fig. 4 and S1).

From our results, HET-LBN mice seem to lack the ability of fine-tuning their exploratory behavior when exposed to a potential threat (falling from the open arm of the EPM), suggesting an impairment in their cognitive-emotional flexibility. Elegant studies showed that the fine-tuning of receptive fields (El-Boustani et al., 2018) or the specificity of associative memories (Wu et al., 2021) benefit of a rebound synaptic downscaling that restores local network dynamics to a critical state (Ma et al., 2019). A highly dynamic synaptic turnover is an ideal feature that allows the maintenance of this homeostasis in local brain circuits (Caroni et al., 2012; El-Boustani et al., 2018; Jenks et al., 2021; Ma et al., 2019; Wen and Turrigiano, 2021; Wu et al., 2020, 2021). We postulate that a similar mechanism may be at play in our model. We hypothesized that lack of synaptic turnover within the BLA may underlie a deteriorated signal-to-noise ratio within the amygdala microcircuitry, determining an over-generalization of behavioral strategies, irrespectively to the biological valence of the environment. In support of this hypothesis, a previous study shows that organized synaptic ensembles identified by immunolabeling of 6-sulfated chondroitin sulfate (Chelini et al., 2023) are reduced in the postmortem brain of people with BD (Pantazopoulos et al., 2015), suggesting that the lack of locally organized plasticity may contribute to psychoses. To test this hypothesis, we asked whether signs of behavioral rigidity may be accompanied by deficient synaptic turnover in the BLA. This brain region works as a multisensory hub, integrating interoceptive and exteroceptive inputs to encode the biological value of external cues, based on adaptive needs (Daviu et al., 2019). Using the size of PSD95 puncta as a proxy for synaptic strength, we found that: i) Early-life adversity promotes the accumulation of larger postsynaptic densities in the BLA at the expense of smaller ones, and that this effect is amplified by *Cntnap2* heterozygous mutation, and ii) Increase postsynaptic density inversely correlates with the preference for safety (Fig. 6). Then, we interrogated the microglia phenotype within the BLA of the same mice. Microglia are major players implicated in activity-dependent synaptic refinement and studies are increasingly showing the contribution of this cell-type in the pathophysiology of psychiatric disorders (Mondelli et al., 2017; Rahimian et al., 2021). Furthermore microglial morphological and functional alterations have been frequently observed across mouse models of neurodevelopmental disorders (Hughes et al., 2023), including *Cntnap2* full knockout mice (Dawson et al., 2023). Our findings show that microglia are affected by *Cntnap2* heterozygous mutation, particularly when challenged with an early-life adverse experience. HET-LBN mice display bigger microglial volume and higher content of CD68-positive phagolysosomes within the BLA, compared to all the other conditions (Fig. 7). Altered CD68 content can be associated with increased or decreased phagocytosis of synapses and cellular debris (Filipello et al., 2018; Monsorno et al., 2023; Paolicelli et al., 2017). However, it remains to be determined whether this modulation is functionally involved in the refinement of synapses and in the behavioral alterations described in this study. Previous studies have described changes in the morphology of microglia, which acquire a hyper-ramified phenotype in response to chronic stress (Hellwig et al., 2016; Hinwood et al., 2013) Of note, these structural alterations were suggested to be crucial for depressive-like behavior development in mice, and were dependent on the Cx3cr1 signaling pathway (Hellwig et al., 2016). The increased size of microglia, along with their higher content of phagolysosomes, which we reported in HET-LBN mice, could indicate a hyperactive microglial state, underlying a potential compensatory remodeling, with consequence on synaptic plasticity. In this study we did not specifically assess the inflammatory response induced by early-life adverse experience, therefore we cannot exclude the contribution of cytokine dysregulation in association with the reported hyper-trophic phenotype. Several studies have indeed confirmed a microglial response and elevated pro-inflammatory cytokine signaling in key brain regions implicated in human psychiatric disorders, following paradigms of early life stress (Dutcher et al., 2020). Therefore,

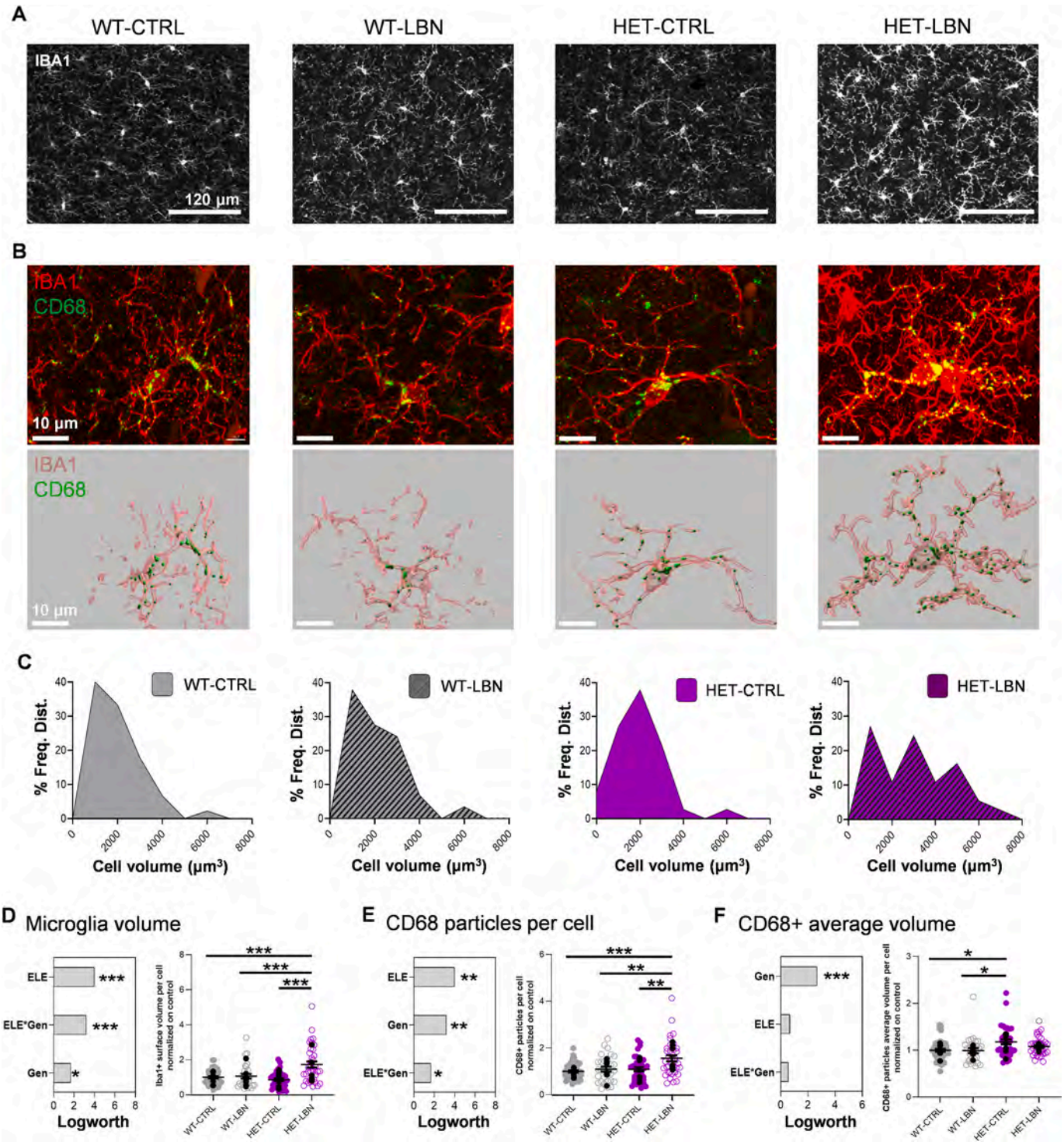

Fig. 7. Altered microglia phenotype in *Cntnap2*$^{+/-}$ mice is worsened by LBN. **(A)** Confocal photomicrographs showing an overview of IBA1-positive microglia cells in BLA. **(B)** Confocal photomicrographs capturing a detailed view of a typical microglia appearance in each of the four experimental groups (top) and paired with its relative 3D reconstruction (bottom). **(C)** Frequency plots showing the distribution of microglia size in the four experimental conditions as revealed by rank analysis; HET-LBN presents with a greater proportion of larger cells (between 4000 and 6000 µm^3) compared to WT-CTRL and HET-CTRL (for visualization purpose, cells were categorized according to size-bins of 1000 µm^3). **(D, E)** Left panels: charts summarizing the quantification of the main effect of the covariates included in the model; Right charts: depict the results of multiple comparisons for the given outcome measure. **(D)** A main effect of both ELE and ELE^{x}Gen is driven by significant increase in the microglia size selective for HET-LBN (as forecast in panel C). **(E)** The number of CD68^{+} phagolysosomes per cell is selectively increased in HET-LBN, determining significant effect of both ELE and Gen and their interaction. **(F)** Conversely, the average volume of CD68-positive phagolysosomes per cell surface area is exclusively affected by CNTNAP2 haploinsufficiency, with significant differences observed between HET-CTRL and both WT groups. Black dots indicate values for single animal. Colored dots indicate values of single cells.
ELE = early-life experience; Gen = genotype; ^{x} indicates interaction. *p < 0.05/**p < 0.001/***p < 0.0001.

further studies are urgently needed to address the functional relevance of this phenotype, and the effects on synapses structure and function. In conclusion, we propose that the mechanisms of homeostatic plasticity are impaired in HET-LBN mice and that this works as a substrate for impaired affective tuning.

Importantly, we confirmed that standard-reared *Cntnap2*$^{+/-}$ mice do not show major behavioral abnormalities compared to wild-type littermates. However, we were able to detect some sub-threshold discrepancies with respect to WT-CTRL (locomotor activity in the L/D, attenuated adaptation in the EPM). Furthermore, the microglia phenotype in HET-CTRL showed some critical differences with WT-CTRL, suggesting that a divergent neural functioning may underlie parallel behavioral strategy that eventually converge to similar behavioral outcomes. Interestingly, similar evidence comes from the study of family members of patients with a psychiatric diagnosis (Zhang et al., 2023): these studies show that undiagnosed first-degree relatives display functional (Arat et al., 2015), molecular (Petersen et al., 2021) and behavioral (Bora and Özerdem, 2017) characteristics overlapping with what observed in their diagnosed family member. In line with these findings, we propose that C*ntnap2* haploinsufficiency may confer a status of subliminal emotional vulnerability that exacerbates maladaptive behaviors as a consequence of adverse childhood experience.

One surprising aspect of this study is the lack of any meaningful impact of sex in the behavioral outcomes of HET-LBN mice. This is despite a significant difference between males and females WT-LBN mice in the L/D boxes; a piece of evidence that corroborates previous findings (Brenhouse and Bath, 2019; Ganguly et al., 2019; Gildawie et al., 2020; Guadagno et al., 2021; Manzano Nieves et al., 2023, 2023, 2023; Walker et al., 2017). One possible interpretation is that a predominant vulnerability conferred by the *Cntnap2* mutation may overshadow the role of sex-differences. However, one alternative explanation may be related to the low statistical power of the study. To spot subtle differences in an 8-group model would require -approximately- twice as many animals; an effort that was not justified by the very low role of sex that emerged from our analysis of covariates. More realistically, it is entirely possible that, while the behavioral domains tested in this work lack any convincing sex-bias in the HET-LBN mice, other domains such as learning and memory or executive functions may be affected. This possibility could be an ideal starting point for future investigation.

Finally, we would like to emphasize a few methodological considerations. One is the importance of using a standardized breeding strategy. This approach is already suggested in previous articles describing the LBN procedure (Walker et al., 2017). In this work, however, it was necessary to control for the effect of maternal genotype. As revealed by our behavioral phenotyping, *Cntnap2*$^{+/-}$ females do show minimal discrepancies with controls that went previously undetected. Thus, there was some chance that the LBN may interact with the maternal genotype differently, preventing us to establish whether behavioral alterations in the offspring are due to the offspring or the mother's genetic background; the use of WT dams eliminated this problem. A second critical point is the inclusion of the factor time in the behavioral evaluation. The time-dependency of symptoms is an integral component of psychopathology (Salvatore et al., 2012; Wirz-Justice, 2007). Especially in mood disorders, symptoms cycle on multiple time-scales, from seasonal (Rosenthal et al., 2020), to circadian (McCarty et al., 2021) up to milliseconds differences in reaction times (Fleck et al., 2001) and discrepancies in time-perception (Mavrogiorgou et al., 2022). In this work we chose to investigate arbitrary time-bins to obtain a behavioral redout indicative of either impulsivity or perseverance, which proved an effective strategy to harness the complexity of some deviant traits. It will be necessary, in future studies, to expand the assessment of time-behavior interaction in preclinical models of psychiatric disorders. A third point that requires care in the interpretation of our results is the potential role of social isolation. All mice were single-housed a few days prior to the beginning of the behavioral battery. This was done to minimize the acute stress derived from home-cage hierarchies during the testing phase (Karamihalev et al., 2020). While this strategy allowed us to equalize the experimental condition across the cohort, it is possible that the week of social isolation exerts some additional impact and contributing to the behavioral outcomes (Matsumoto et al., 2019).

The current study primarily focuses on the quantification of stress and anxiety while also glancing at autistic-like behaviors; further studies will be needed to disentangle the complexity of altered emotion regulation in HET-LBN mice. For instance, a deep evaluation of signs of mood dysregulation, cognitive flexibility or reward-seeking will be integral to verify the translational validity of this two-hit model to investigate the biological underpinnings of disorders such as schizophrenia or bipolar disorders. Furthermore, synaptic and microglia anomalies in the BLA are -most likely-just the tip of the iceberg of a broader scale impact of LBN onto *Cntnap2*$^{+/}$. Ideally, future studies will shed light on which brain systems are affected, how gene-environment interaction influences local and broad-scale connectivity, and whether (and to what extent) certain types of neurons are impacted. As many questions remain open, we emphasize that by delivering a timely application of an early environmental stressor we unravel part of the phenotypic heterogeneity associated with C*ntnap2* haploinsufficiency, showing that this mutation may constitute a causal factor for certain psychiatric symptoms only and exclusively when associated with specific environmental risks, such as prenatal immune activation (Haddad et al., 2023) or early-life adverse experiences.

CRediT authorship contribution statement

Gabriele Chelini: Writing – review & editing, Writing – original draft, Validation, Supervision, Resources, Methodology, Investigation, Funding acquisition, Formal analysis, Data curation, Conceptualization. **Tommaso Fortunato-Asquini:** Investigation. **Enrica Cerilli:** Investigation. **Katia Monsorno:** Writing – review & editing, Investigation, Data curation. **Benedetta Catena:** Investigation. **Ginevra Matilde Dall'O':** Investigation. **Rosa Chiara Paolicelli:** Writing – review & editing, Validation, Supervision, Resources. **Yuri Bozzi:** Writing – review & editing, Validation, Supervision, Resources, Project administration, Conceptualization.

Funding

GC effort was covered by the 'CARITRO postdoctoral fellowship', funded by Fondazione Cassa di Risparmio di Trento e Rovereto and the University of Trento starting grant, provided by the University of Trento. GC acknowledges funding from Next Generation EU, in the context of the National Recovery and Resilience Plan, Investment PE8 – Project Age-It: "Ageing Well in an Ageing Society" [DM 1557 October 11, 2022]. YB was supported by the Strategic Project TRAIN - Trentino Autism Initiative from the University of Trento (grant 2018-2022). RCP was supported by grants from ERC (StGrant REMIND 804949), SNSF (SNSF 310030_197940) and funding from UNIL.

Declaration of competing interest

The authors declare no competing interests.

Acknowledgments

We thank all the administrative and technical staff of CIMeC for support. A special thank goes to Mrs. Michela Maffei, animal caretaker of the CIMeC animal facility, for her endless care and support provided in managing the animal colony used in the study and Dr. Tommaso Pecchia for helping with the technical implementations of some of the behavioral apparatuses.

Appendix A. Supplementary data

Supplementary data to this article can be found online at https://doi.org/10.1016/j.ynstr.2025.100726.

Data availability

Data will be made available on request.

References

American Psychiatric Association, 2022. Diagnostic and Statistical Manual of Mental Disorders, Fifth Edition. American Psychiatric Publishing, Washington, DC, USA. Text Revision (DSM-5-TR), ISBN 978-0-89042-575-6.

Angoa-Pérez, M., Kane, M.J., Briggs, D.I., Francescutti, D.M., Kuhn, D.M., 2013. Marble burying and nestlet shredding as tests of repetitive, compulsive-like behaviors in mice. JoVE J. 50978. https://doi.org/10.3791/50978.

Arat, H.E., Chouinard, V.-A., Cohen, B.M., Lewandowski, K.E., Öngür, D., 2015. Diffusion tensor imaging in first degree relatives of schizophrenia and bipolar disorder patients. Schizophr. Res. 161, 329–339. https://doi.org/10.1016/j.schres.2014.12.008.

Bagheri, F., Goudarzi, I., Lashkarbolouki, T., Elahdadi Salmani, M., Goudarzi, A., Morley-Fletcher, S., 2022. The combined effects of perinatal ethanol and early-life stress on cognition and risk-taking behavior through oxidative stress in rats. Neurotox. Res. 40, 925–940. https://doi.org/10.1007/s12640-022-00506-6.

Bora, E., Özerdem, A., 2017. Social cognition in first-degree relatives of patients with bipolar disorder: a meta-analysis. Eur. Neuropsychopharmacol. 27, 293–300. https://doi.org/10.1016/j.euroneuro.2017.02.009.

Brenhouse, H.C., Bath, K.G., 2019. Bundling the haystack to find the needle: challenges and opportunities in modeling risk and resilience following early life stress. Front. Neuroendocrinol. 54, 100768. https://doi.org/10.1016/j.yfrne.2019.100768.

Canali, G., Goutebroze, L., 2018. *CNTNAP2* heterozygous missense variants: risk factors for autism spectrum disorder and/or other pathologies? J. Exp. Neurosci. 12, 117906951880966. https://doi.org/10.1177/1179069518809666.

Caroni, P., Donato, F., Muller, D., 2012. Structural plasticity upon learning: regulation and functions. Nat. Rev. Neurosci. 13, 478–490. https://doi.org/10.1038/nrn3258.

Caspi, A., Moffitt, T.E., 2006. Gene–environment interactions in psychiatry: joining forces with neuroscience. Nat. Rev. Neurosci. 7, 583–590. https://doi.org/10.1038/nrn1925.

Chelini, G., Mirzapourdelavar, H., Durning, P., Baidoe-Ansah, D., O'Donovan, S.M., Klengel, T., Balasco, L., Berciu, C., Boyer-Boiteau, A., Smith, R., Ressler, K.J., Bozzi, Y., Dityatev, A., Berretta, S., 2023. Focal clusters of peri-synaptic matrix contribute to activity-dependent plasticity and memory (preprint). SSRN. https://doi.org/10.2139/ssrn.4512954.

Chelini, G., Pangrazzi, L., Bozzi, Y., 2022. At the crossroad between resiliency and fragility: a neurodevelopmental perspective on early-life experiences. Front. Cell. Neurosci. 16, 863866. https://doi.org/10.3389/fncel.2022.863866.

Daviu, N., Bruchas, M.R., Moghaddam, B., Sandi, C., Beyeler, A., 2019. Neurobiological links between stress and anxiety. Neurobiol. Stress 11, 100191. https://doi.org/10.1016/j.ynstr.2019.100191.

Dawson, M.S., Gordon-Fleet, K., Yan, L., Tardos, V., He, H., Mui, K., Nawani, S., Asgarian, Z., Catani, M., Fernandes, C., Drescher, U., 2023. Sexual dimorphism in the social behaviour of Cntnap2-null mice correlates with disrupted synaptic connectivity and increased microglial activity in the anterior cingulate cortex. Commun. Biol. 6, 846. https://doi.org/10.1038/s42003-023-05215-0.

Dutcher, E.G., Pama, E.A.C., Lynall, M.-E., Khan, S., Clatworthy, M.R., Robbins, T.W., Bullmore, E.T., Dalley, J.W., 2020. Early-life stress and inflammation: a systematic review of a key experimental approach in rodents. Brain Neurosci. Adv. 4, 239821282097804. https://doi.org/10.1177/2398212820978049.

El-Boustani, S., Ip, J.P.K., Breton-Provencher, V., Knott, G.W., Okuno, H., Bito, H., Sur, M., 2018. Locally coordinated synaptic plasticity of visual cortex neurons in vivo. Science 360, 1349–1354. https://doi.org/10.1126/science.aao0862.

Filipello, F., Morini, R., Corradini, I., Zerbi, V., Canzi, A., Michalski, B., Erreni, M., Markicevic, M., Starvaggi-Cucuzza, C., Otero, K., Piccio, L., Cignarella, F., Perrucci, F., Tamborini, M., Genua, M., Rajendran, L., Menna, E., Vetrano, S., Fahnestock, M., Paolicelli, R.C., Matteoli, M., 2018. The microglial innate immune receptor TREM2 is required for synapse elimination and normal brain connectivity. Immunity 48, 979–991.e8. https://doi.org/10.1016/j.immuni.2018.04.016.

Fleck, D.E., Sax, K.W., Strakowski, S.M., 2001. Reaction time measures of sustained attention differentiate bipolar disorder from schizophrenia. Schizophr. Res. 52, 251–259. https://doi.org/10.1016/S0920-9964(01)00170-0.

Florén Lind, S., Stam, F., Zelleroth, S., Meurling, E., Frick, A., Grönbladh, A., 2023. Acute caffeine differently affects risk-taking and the expression of BDNF and of adenosine and opioid receptors in rats with high or low anxiety-like behavior. Pharmacol. Biochem. Behav. 227–228, 173573. https://doi.org/10.1016/j.pbb.2023.173573.

Ganguly, P., Honeycutt, J.A., Rowe, J.R., Demaestri, C., Brenhouse, H.C., 2019. Effects of early life stress on cocaine conditioning and AMPA receptor composition are sex-specific and driven by TNF. Brain Behav. Immun. 78, 41–51. https://doi.org/10.1016/j.bbi.2019.01.006.

Gildawie, K.R., Honeycutt, J.A., Brenhouse, H.C., 2020. Region-specific effects of maternal separation on perineuronal net and parvalbumin-expressing interneuron formation in male and female rats. Neuroscience 428, 23–37. https://doi.org/10.1016/j.neuroscience.2019.12.010.

Guadagno, A., Belliveau, C., Mechawar, N., Walker, C.-D., 2021. Effects of early life stress on the developing basolateral amygdala-prefrontal cortex circuit: the emerging role of local inhibition and perineuronal nets. Front. Hum. Neurosci. 15, 669120. https://doi.org/10.3389/fnhum.2021.669120.

Haddad, F.L., De Oliveira, C., Schmid, S., 2023. Investigating behavioral phenotypes related to autism spectrum disorder in a gene-environment interaction model of Cntnap2 deficiency and Poly I:C maternal immune activation. Front. Neurosci. 17, 1160243. https://doi.org/10.3389/fnins.2023.1160243.

Hellwig, S., Brioschi, S., Dieni, S., Frings, L., Masuch, A., Blank, T., Biber, K., 2016. Altered microglia morphology and higher resilience to stress-induced depression-like behavior in CX3CR1-deficient mice. Brain Behav. Immun. 55, 126–137. https://doi.org/10.1016/j.bbi.2015.11.008.

Hinwood, M., Tynan, R.J., Charnley, J.L., Beynon, S.B., Day, T.A., Walker, F.R., 2013. Chronic stress induced remodeling of the prefrontal cortex: structural Re-organization of microglia and the inhibitory effect of minocycline. Cerebr. Cortex 23, 1784–1797. https://doi.org/10.1093/cercor/bhs151.

Hughes, H.K., Moreno, R.J., Ashwood, P., 2023. Innate immune dysfunction and neuroinflammation in autism spectrum disorder (ASD). Brain Behav. Immun. 108, 245–254. https://doi.org/10.1016/j.bbi.2022.12.001.

Jenks, K.R., Tsimring, K., Ip, J.P.K., Zepeda, J.C., Sur, M., 2021. Heterosynaptic plasticity and the experience-dependent refinement of developing neuronal circuits. Front. Neural Circ. 15, 803401. https://doi.org/10.3389/fncir.2021.803401.

Ji, W., Li, T., Pan, Y., Tao, H., Ju, K., Wen, Z., Fu, Y., An, Z., Zhao, Q., Wang, T., He, L., Feng, G., Yi, Q., Shi, Y., 2013. CNTNAP2 is significantly associated with schizophrenia and major depression in the Han Chinese population. Psychiatry Res. 207, 225–228. https://doi.org/10.1016/j.psychres.2012.09.024.

Kaidanovich-Beilin, O., Lipina, T., Vukobradovic, I., Roder, J., Woodgett, J.R., 2011. Assessment of social interaction behaviors. JoVE J. 2473. https://doi.org/10.3791/2473.

Karamihalev, S., Brivio, E., Flachskamm, C., Stoffel, R., Schmidt, M.V., Chen, A., 2020. Social dominance mediates behavioral adaptation to chronic stress in a sex-specific manner. Elife 9, e58723. https://doi.org/10.7554/eLife.58723.

Komada, M., Takao, K., Miyakawa, T., 2008. Elevated plus maze for mice. JoVE J. 1088. https://doi.org/10.3791/1088.

Kraeuter, A.-K., Guest, P.C., Sarnyai, Z., 2019. The open field test for measuring locomotor activity and anxiety-like behavior. In: Guest, P.C. (Ed.), Pre-Clinical Models, Methods in Molecular Biology. Springer, New York, New York, NY, pp. 99–103. https://doi.org/10.1007/978-1-4939-8994-2_9.

Lukens, J.R., Eyo, U.B., 2022. Microglia and neurodevelopmental disorders. Annu. Rev. Neurosci. 45, 425–445. https://doi.org/10.1146/annurev-neuro-110920-023056.

Ma, Z., Turrigiano, G.G., Wessel, R., Hengen, K.B., 2019. Cortical circuit dynamics are homeostatically tuned to criticality in vivo. Neuron 104, 655–664.e4. https://doi.org/10.1016/j.neuron.2019.08.031.

Manzano Nieves, G., Bravo, M., Baskoylu, S., Bath, K.G., 2020. Early life adversity decreases pre-adolescent fear expression by accelerating amygdala PV cell development. Elife 9, e55263. https://doi.org/10.7554/eLife.55263.

Manzano Nieves, G., Bravo, M., Bath, K.G., 2023. Early life adversity ablates sex differences in active versus passive threat responding in mice. Stress 26, 2244598. https://doi.org/10.1080/10253890.2023.2244598.

Matsumoto, K., Fujiwara, H., Araki, R., Yabe, T., 2019. Post-weaning social isolation of mice: a putative animal model of developmental disorders. J. Pharmacol. Sci. 141, 111–118. https://doi.org/10.1016/j.jphs.2019.10.002.

Mavrogiorgou, P., Thomaßen, T., Pott, F., Flasbeck, V., Steinfath, H., Juckel, G., 2022. Time experience in patients with schizophrenia and affective disorders. Eur. Psychiatry 65, e11. https://doi.org/10.1192/j.eurpsy.2022.2.

McCarty, R., Josephs, T., Kovtun, O., Rosenthal, S.J., 2021. Enlightened: addressing circadian and seasonal changes in photoperiod in animal models of bipolar disorder. Transl. Psychiatry 11, 373. https://doi.org/10.1038/s41398-021-01494-5.

Mondelli, V., Vernon, A.C., Turkheimer, F., Dazzan, P., Pariante, C.M., 2017. Brain microglia in psychiatric disorders. Lancet Psychiatry 4, 563–572. https://doi.org/10.1016/S2215-0366(17)30101-3.

Monsorno, K., Ginggen, K., Ivanov, A., Buckinx, A., Lalive, A.L., Tchenio, A., Benson, S., Vendrell, M., D'Alessandro, A., Beule, D., Pellerin, L., Mameli, M., Paolicelli, R.C., 2023. Loss of microglial MCT4 leads to defective synaptic pruning and anxiety-like behavior in mice. Nat. Commun. 14, 5749. https://doi.org/10.1038/s41467-023-41502-4.

Musci, R.J., Augustinavicius, J.L., Volk, H., 2019. Gene-environment interactions in psychiatry: recent evidence and clinical implications. Curr. Psychiatry Rep. 21, 81. https://doi.org/10.1007/s11920-019-1065-5.

ODushlaine, C., Kenny, E., Heron, E., Donohoe, G., Gill, M., Morris, D., Corvin, A., 2011. Molecular pathways involved in neuronal cell adhesion and membrane scaffolding contribute to schizophrenia and bipolar disorder susceptibility. Mol. Psychiatr. 16, 286–292. https://doi.org/10.1038/mp.2010.7.

Pantazopoulos, H., Markota, M., Jaquet, F., Ghosh, D., Wallin, A., Santos, A., Caterson, B., , The International Schizophrenia Consortium, Berretta, S., 2015. Aggrecan and chondroitin-6-sulfate abnormalities in schizophrenia and bipolar disorder: a postmortem study on the amygdala. Transl. Psychiatry 5, e496. https://doi.org/10.1038/tp.2014.128 e496.

Paolicelli, R.C., Jawaid, A., Henstridge, C.M., Valeri, A., Merlini, M., Robinson, J.L., Lee, E.B., Rose, J., Appel, S., Lee, V.M.-Y., Trojanowski, J.Q., Spires-Jones, T., Schulz, P.E., Rajendran, L., 2017. TDP-43 depletion in microglia promotes amyloid clearance but also induces synapse loss. Neuron 95, 297–308.e6. https://doi.org/10.1016/j.neuron.2017.05.037.

Peñagarikano, O., Abrahams, B.S., Herman, E.I., Winden, K.D., Gdalyahu, A., Dong, H., Sonnenblick, L.I., Gruver, R., Almajano, J., Bragin, A., Golshani, P., Trachtenberg, J. T., Peles, E., Geschwind, D.H., 2011. Absence of CNTNAP2 leads to epilepsy,

neuronal migration abnormalities, and core autism-related deficits. Cell 147, 235–246. https://doi.org/10.1016/j.cell.2011.08.040.
Peñagarikano, O., Lázaro, M.T., Lu, X.-H., Gordon, A., Dong, H., Lam, H.A., Peles, E., Maidment, N.T., Murphy, N.P., Yang, X.W., Golshani, P., Geschwind, D.H., 2015. Exogenous and evoked oxytocin restores social behavior in the *Cntnap2* mouse model of autism. Sci. Transl. Med. 7. https://doi.org/10.1126/scitranslmed.3010257.
Petersen, N.A., Nielsen, M.Ø., Coello, K., Stanislaus, S., Melbye, S., Kjærstad, H.L., Sletved, K.S.O., McIntyre, R.S., Frikke-Smith, R., Vinberg, M., Kessing, L.V., 2021. Brain-derived neurotrophic factor levels in newly diagnosed patients with bipolar disorder, their unaffected first-degree relatives and healthy controls. BJPsych open 7, e55. https://doi.org/10.1192/bjo.2021.9.
Rahimian, R., Wakid, M., O'Leary, L.A., Mechawar, N., 2021. The emerging tale of microglia in psychiatric disorders. Neurosci. Biobehav. Rev. 131, 1–29. https://doi.org/10.1016/j.neubiorev.2021.09.023.
Reshetnikov, V.V., Ayriyants, K.A., Ryabushkina, Y.A., Sozonov, N.G., Bondar, N.P., 2021. Sex-specific behavioral and structural alterations caused by early-life stress in C57BL/6 and BTBR mice. Behav. Brain Res. 414, 113489. https://doi.org/10.1016/j.bbr.2021.113489.
Rodenas-Cuadrado, P., Pietrafusa, N., Francavilla, T., La Neve, A., Striano, P., Vernes, S. C., 2016. Characterisation of CASPR2 deficiency disorder - a syndrome involving autism, epilepsy and language impairment. BMC Med. Genet. 17, 8. https://doi.org/10.1186/s12881-016-0272-8.
Rosenthal, S.J., Josephs, T., Kovtun, O., McCarty, R., 2020. Seasonal effects on bipolar disorder: a closer look. Neurosci. Biobehav. Rev. 115, 199–219. https://doi.org/10.1016/j.neubiorev.2020.05.017.
Salvatore, P., Indic, P., Murray, G., Baldessarini, R.J., 2012. Biological rhythms and mood disorders. Dialogues Clin. Neurosci. 14, 369–379. https://doi.org/10.31887/DCNS.2012.14.4/psalvatore.
Schneider, C.A., Rasband, W.S., Eliceiri, K.W., 2012. NIH Image to ImageJ: 25 years of image analysis. Nat. Methods 9, 671–675. https://doi.org/10.1038/nmeth.2089.
Scott, K.E., Kazazian, K., Mann, R.S., Möhrle, D., Schormans, A.L., Schmid, S., Allman, B. L., 2020. Loss of *Cntnap2* in the rat causes autism-related alterations in social interactions, stereotypic behavior, and sensory processing. Autism Res. 13, 1698–1717. https://doi.org/10.1002/aur.2364.
Takao, K., Miyakawa, T., 2006. Light/dark transition test for mice. JoVE J. 104. https://doi.org/10.3791/104.
Thorndike, R.L., 1953. Who belongs in the family? Psychometrika 18, 267–276. https://doi.org/10.1007/BF02289263.
Toma, C., Pierce, K.D., Shaw, A.D., Heath, A., Mitchell, P.B., Schofield, P.R., Fullerton, J. M., 2018. Comprehensive cross-disorder analyses of CNTNAP2 suggest it is unlikely to be a primary risk gene for psychiatric disorders. PLoS Genet. 14, e1007535. https://doi.org/10.1371/journal.pgen.1007535.
Walker, C.-D., Bath, K.G., Joels, M., Korosi, A., Larauche, M., Lucassen, P.J., Morris, M.J., Raineki, C., Roth, T.L., Sullivan, R.M., Taché, Y., Baram, T.Z., 2017. Chronic early life stress induced by limited bedding and nesting (LBN) material in rodents: critical considerations of methodology, outcomes and translational potential. Stress 20, 421–448. https://doi.org/10.1080/10253890.2017.1343296.
Wang, K.-S., Liu, X.-F., Aragam, N., 2010. A genome-wide meta-analysis identifies novel loci associated with schizophrenia and bipolar disorder. Schizophr. Res. 124, 192–199. https://doi.org/10.1016/j.schres.2010.09.002.
Wen, W., Turrigiano, G.G., 2021. Developmental regulation of homeostatic plasticity in mouse primary visual cortex. J. Neurosci. 41, 9891–9905. https://doi.org/10.1523/JNEUROSCI.1200-21.2021.
Wirz-Justice, A., 2007. Chronobiology and psychiatry. Sleep Med. Rev. 11, 423–427. https://doi.org/10.1016/j.smrv.2007.08.003.
Wu, C.-H., Ramos, R., Katz, D.B., Turrigiano, G.G., 2021. Homeostatic synaptic scaling establishes the specificity of an associative memory. Curr. Biol. 31, 2274–2285.e5. https://doi.org/10.1016/j.cub.2021.03.024.
Wu, Y.K., Hengen, K.B., Turrigiano, G.G., Gjorgjieva, J., 2020. Homeostatic mechanisms regulate distinct aspects of cortical circuit dynamics. Natl. Acad. Sci. U.S.A 117, 24514–24525. https://doi.org/10.1073/pnas.1918368117.
Zhan, Y., Paolicelli, R.C., Sforazzini, F., Weinhard, L., Bolasco, G., Pagani, F., Vyssotski, A.L., Bifone, A., Gozzi, A., Ragozzino, D., Gross, C.T., 2014. Deficient neuron-microglia signaling results in impaired functional brain connectivity and social behavior. Nat. Neurosci. 17, 400–406. https://doi.org/10.1038/nn.3641.
Zhang, H., Chen, J., Fang, Y., 2023. Functional alterations in patients with bipolar disorder and their unaffected first-degree relatives: insight from genetic, epidemiological, and neuroimaging data. NDT 19, 2797–2806. https://doi.org/10.2147/NDT.S427617.